



fields, especially for use as composite fillers in polymers to improve the mechanical, thermal, and electrical properties of resulting composites. There have been indications of a number of potential applications for CNTs, including microwave absorption,<sup>6,7</sup> corrosion protection,<sup>8,9</sup> reinforced materials in natural fibre composites,<sup>10,11</sup> electromagnetic interference shielding (EMI),<sup>12,13</sup> batteries,<sup>14,15</sup> solar cells,<sup>16–19</sup> chemical sensor,<sup>20–23</sup> hydrogen storage,<sup>24,25</sup> and field-emission materials.<sup>26,27</sup> Other than CNTs, Chen and Shao (2016) had listed other types of carbonaceous materials, such as amorphous porous carbon, graphene, carbon black, carbon nanofibre, and graphite.<sup>28,29</sup> Due to their superior and unique electronic properties, inert properties of carbonaceous materials are widely used as counter electrodes (CE).<sup>30–34</sup> Their advantage and limitations on the structural and electronic properties of the listed carbonaceous materials are summarised in Table 1.

The physical and catalytic properties of CNTs make it ideal to be used in chemical sensors. Most notably, the high degree of organisation and high aspect ratio of CNTs has pronounced excellent chemical, thermal, and mechanical properties in terms of stiffness, Young's modulus, flexibility, and electrical conductivity.<sup>43–46</sup> The remarkable properties of CNTs are useful for constructing nanoscale devices and developing multifunctional composite materials.<sup>47–49</sup> The two main types of CNTs are single-walled CNTs (SWCNTs) and multi-walled carbon nanotubes (MWCNTs) (Fig. 1). SWCNTs are  $sp^2$  hybridised carbon in a hexagonal honeycomb structure that is rolled into a hollow tube morphology, while MWCNTs are multiple concentric tubes encircling one another.<sup>50</sup> Recently, CNTs have started to attract ever increasing interest as a conductive filler and reinforcement for polymeric composites. Apart from high electrical conductivity, CNTs also have unique electronic and optical properties for development of organoelectronic devices.<sup>51,52</sup> The possibility to achieve reasonably high conductivity at very low CNT concentration, between 0.0025 and 4 wt%, is owed to its high aspect ratio ( $L/D$ , where  $L$  is length of CNT and  $D$  is diameter of CNT) from 100 to 1000, which makes them an ideal candidate to be harnessed for several potential applications especially in electronic devices and structural components. Such high aspect ratio facilitates CNT to form a 'network-like' structure in the composites at a particular low concentration termed as percolation.<sup>53</sup> In other words, increase in CNT concentration/loading usually results in transition from a poor-conducting state to a good conducting state at a certain threshold volume fraction of the conductive filler. The volume fraction of CNTs, necessary for building a continuous conductive path inside the polymer matrix, is referred to as the percolation threshold. It seems promising to prepare the materials with small content and ratio which preserve the desired mechanical properties of a polymer along with a higher electrical conductivity.<sup>54</sup> Fig. 2(c) shows the transmission electron microscopy (TEM) of purified MWCNTs with long intertwined CNTs. As observed, the obtained CNTs with diameter of about 20 nm were clean, and almost all impurities have been removed without destroying the basic structure of the nanotubes.<sup>55</sup>

Numerous other CNT forms, such as double-walled CNTs,<sup>56</sup> bamboo,<sup>57</sup> and herringbone<sup>58</sup> have also been synthesised and

discovered. The nanostructure of CNTs has been reviewed by Delgado *et al.* (2007), where fullerenes and CNTs are only the tip of the iceberg and, more recently, a wide variety of new carbon nanostructures, such as endohedral fullerenes, cup-stacked nanotubes, nanohorns, nanotori, nanobuds, and nanooxions, have emerged as new and fascinating forms of carbon. The chemical and physical properties of these new forms of carbon are currently being unravelled.<sup>59</sup> SWCNTs can be classified as either semi-conducting or metallic allotropes, depending on the chirality. The distinction of semi-conducting or metallic is important for their use in different sensors, but the physical separation of allotropes has proven to be one of the more difficult challenges to overcome. In MWCNTs, a single metallic layer results in the entire nanotube displaying metallic behaviour. Fig. 2(a) shows the structure of MWCNTs made up of three shells of different chirality, while Fig. 2(b) shows the formation of SWCNTs through the roll-up of graphene with respect to the hexagonal lattice sheet leading to the three different types of CNTs.

The recent discovery on CNTs also has attracted considerable attention due to their dimensions and structure-sensitive properties. The high electrical conductivity of these nanostructures allows the utilisation of CNTs as electrode material, and in combination with its strong electrocatalytic activity offers the ability to mediate electron transfer reactions.<sup>61,62</sup> The facility of electron transfer between the electroactive species and the electrode offers great promise especially for fabricating chemical sensors.<sup>63</sup> Referring to Jacobs *et al.* (2010), the uniqueness of CNTs leads to enhancement of electronic properties, a large edge plane/basal plane ratio, and rapid electrode kinetics. Therefore, CNT-based sensors generally have higher sensitivity, lower limits of detection (LOD), and faster electron transfer kinetics than traditional carbon electrodes.<sup>64</sup>

Besides the aforementioned superior properties of CNTs, owing to the rigidity, chemical inertness, and strong  $\pi$ - $\pi$  interactions of nanotubes, pure CNTs cannot be processed, as they are difficult to dissolve or disperse in common volatile organic solvents (VOS) or polymeric matrices. Due to van der Waals forces of CNTs, the nanotubes tend to agglomerate with each other which results in difficulty of dispersion. In addition to the size effect of CNTs, the physical nature of particles also plays an important role in dispersing them into a polymer matrix. As produced CNTs are held together in bundles or entanglements consisting of 50 to a few hundred individual CNTs by van der Waals force.<sup>65</sup> It has been proven that these bundles and agglomerates result in diminished mechanical and electrical properties of composites as compared with theoretical predictions related to individual CNTs.<sup>66,67</sup> The challenge is on how to incorporate individual CNTs, or at least relatively thin CNT bundles or disentangled CNTs, inside a polymer matrix. In other words, dispersion of CNTs is not only a geometrical problem, which is dealing with the length and size of the CNTs, but also relates to a method on how to separate individual CNTs from CNT agglomerates and stabilise them in a polymer matrix to avoid secondary agglomeration.

Therefore, the side walls of CNTs must be chemically modified to improve their dispersion or solubility in solvents or



Table 1 The structural and electronic properties of various carbonaceous materials

Carbon materials	Advantages	Limitations	Structural	Electrical	Ref.
Amorphous porous carbon	High surface area, advanced porous system, abundant defective sites, superior chemical inertness	Relative low conductivity, poor adhesion with FTO	Consists of an outer spherical shell with porous interior structure, a covalent random network composed of $sp^3$ and $sp^2$ hybridised carbons without grain boundaries, non-crystalline	High electronic conductivity and high surface area, electronic conductivity and ionic conductivity, with specific capacities of $212 \text{ mA h g}^{-1}$ and $162 \text{ mA h g}^{-1}$ at 0.5C and 1C, respectively	35
Graphene	Excellent conductivity, fast charged carrier mobility, good mechanical strength, high optical transparency, good mechanical inertness	Low surface area arising from the easy aggregation, low quantities of defective sites	Crystalline carbon materials, monolayers of carbon atoms arranged in a honeycomb network, giant aromatic macromolecule	Conducts both electricity and heat, thermal conductivity and mechanical stiffness ( $3000 \text{ W m}^{-1} \text{ K}^{-1}$ and $1060 \text{ GPa}$ , respectively)	36
Graphite	Good conductivity, corrosion resistance, excellent thermal stability	Poor porous system, low surface area	Stacks of graphene layers, weak interactions that hold the graphene sheets together	High electrical and thermal conductivity, thermal conductivity 25 to $470 \text{ W m}^{-1} \text{ K}^{-1}$ , electrical resistivity $5 \times 10^{-4}$ to $30 \times 10^{-4} \Omega \text{ cm}$	37 and 38
Carbon black	Plentiful defective sites, good chemical inertness	Low surface area, inappropriate pore size, inadequate conductivity	Typical particle sizes range from around 8 to 100 nm for furnace blacks	Highly structured carbon blacks provide higher viscosity, greater electrical conductivity and easier dispersion for specialty carbon blacks, electrical volume resistivity between 1 to $106 \Omega \text{ cm}$	39
Carbon nanofibre	Excellent mechanical strength, high thermal conductivity, good chemical inertness	Insufficient conductivity, low surface area, inferior porous system	Cylindrical nanostructures with graphene layers arranged as stacked cones, cups or plates, diameters from 50 to 200 nm	High electrical conductivity, and high thermal conductivity, intrinsic conductivity, at room temperature to be $5 \times 10^{-5} \Omega \text{ cm}$	40 and 41
Carbon nanotube	Large surface area, high electrical conductivity, good chemical inertness	Low quantities of defective sites	Crystalline carbon materials, most of the physical properties of carbon nanotubes derive from graphene, carbon atoms are densely organised in a regular $sp^2$ -bonded atomic-scale honeycomb (hexagonal) pattern, $sp^2$ hybridization of carbon builds a layered construction with weak out-of-plane bonding of the van der Waals form and strong in-plane bounds	High electrical conductivity, high thermal conductivity, resistivity of the SWCNT is $10^{-4} \Omega \text{ cm}$ at $27^\circ \text{C}$ , the SWCNT ropes able to sustain much higher stable current densities, as high as $10^{13} \text{ A cm}^{-2}$	41 and 42





Fig. 1 Nanostructures of SWCNTs and MWCNTs, fullerenes and a carbon nano-onion (CNO). Reproduced with permission from ref. 60, copyright 2008, RSC.

polymers, and improve the interaction and reactivity with the polymer by hydrogen bonding interaction.<sup>68</sup> Besides that, altering the surface of nanotubes strongly affects solubility properties, which can affect the ease of fabrication of CNT sensors.<sup>64</sup> As reviewed by Zhao and Stoddart (2009), the non-covalent functionalisation by small molecules, grafting to or wrapping nanotubes with polymers can also alter the

electrochemical properties of the material itself.<sup>69</sup> In mechanical properties enhancement, the incorporation of chemical functionalised CNTs into such polymer enables chemical covalent bonding between the SWCNTs/MWCNTs and the material of interest. Examples of such covalent linkages achieved through chemical functionalisation have been utilised in SWCNT reinforced polymer composites.<sup>70,71</sup> In addition,



Fig. 2 (a) Structure of a multi-walled carbon nanotube made up of three shells of hexagonal lattice sheet of different chirality, (b) roll-up of a graphene sheet that leads to three different types of CNTs and (c) image of purified MWNTs with carboxylation functionalisation under TEM. Reproduced with permission from ref. 55, copyright 2011, *Composites Part A: Applied Science and Manufacturing*.





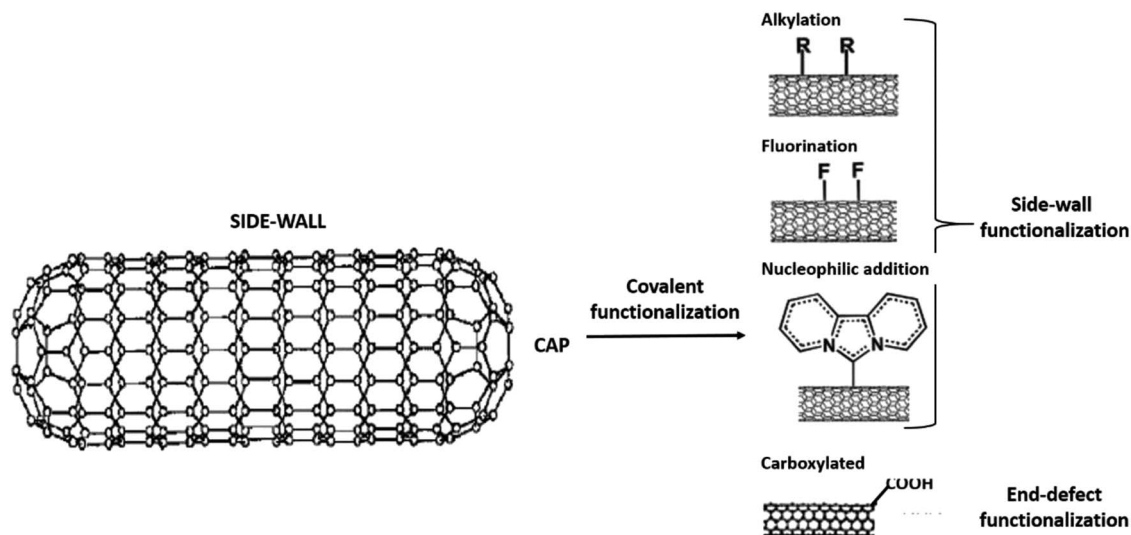


Fig. 3 The covalent functionalisation phenomena at the side and end-cap of CNT structure. Adapted from ref. 77, copyright 2015, Elsevier.

chemical functionalisation is used to enhance the nanotube-polymer interface. Increasing the interfacial bonding between SWCNTs and the polymer will improve the interfacial strength and thus improves load transfer mechanism to the SWCNTs, with the goal of improving the macro and microscopic mechanical properties of the composite system.<sup>72</sup>

Several methods of functionalisation involve chemical,<sup>73</sup> electrochemical,<sup>74</sup> mechano-chemical,<sup>75</sup> and plasma treatment.<sup>76</sup> The functionalisation of CNTs may be treated to functionalise their surfaces and side chain. In chemical functionalisation, the most common treatment with strong acids removes the end caps and also shorten the length of the

CNTs. Acid treatment also adds oxide groups, primarily carboxylic acids, carbonyl, and hydroxyl groups to the tube ends and defect sites of CNTs (Fig. 3).<sup>77</sup> Further chemical reactions can be performed on these oxide groups to functionalise with groups such as amides, thiols, or other groups.<sup>78–80</sup> Balasubramanian and Burghard also had clustered the method of covalent functionalisation of SWCNTs that was accomplished through three different approaches, namely, thermally activated chemistry, electrochemical modification, and photochemical functionalisation.<sup>81</sup> Fig. 4 shows the different methods of functionalisation of CNTs.<sup>82,83</sup>

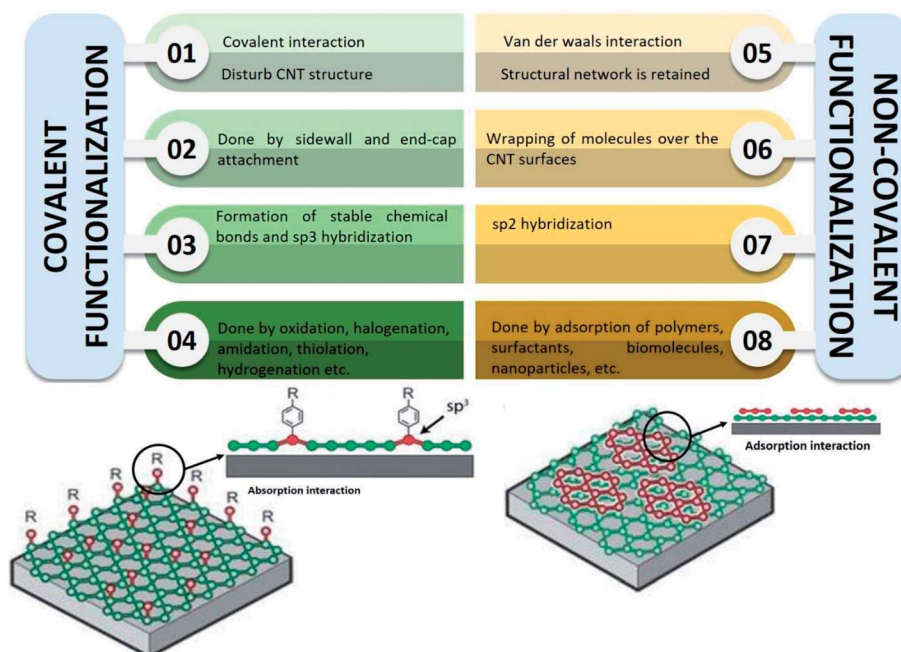


Fig. 4 Comparison between covalent and non-covalent functionalisation of CNTs. Adapted from ref. 36, copyright 2015, Elsevier. And adapted from ref. 37, copyright 2015, Elsevier.



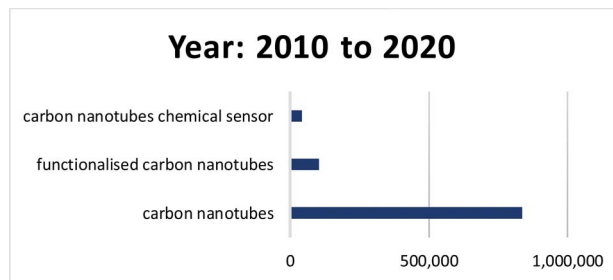


Fig. 5 Number of publications with the specific keywords from the year 2010 to 2020.

Here, a review of recent research towards the development of functionalised CNT-based sensors for the detection of chemical analytes is reviewed. Because of the breadth of research that has been published in this area, this review is only limited to recent publications within the past ten years, 2010 to 2020 (Fig. 5). For that past ten years, about 837 000 publications related to the keyword “carbon nanotubes”, and about 103 000 publications related to the keyword “functionalised carbon nanotubes” were found in Google Scholar (6<sup>th</sup> November 2020). In addition, about 43 700 publications related to “carbon nanotubes chemical sensor” were found. In Malaysia, about 121 publications related to the keyword “carbon nanotubes chemical sensor” were found (data extracted from <http://www.lens.org> on 6<sup>th</sup> November 2020). These findings indicate that CNTs is an interesting subject to be studied, and many more explorations can be done that could lead to huge impacts to the nation. This paper elaborates on the fundamental of CNTs, the covalent and non-covalent functionalisation involved for CNTs, types of analytes, applications of CNTs in sensors, and future perspectives for functionalised CNTs in chemical sensors application.

## 2. Covalent functionalisation of CNTs

Covalent functionalisation of CNTs can be achieved by either direct addition reactions of functional groups or the “active agents” to the sidewalls of nanotubes or modification of appropriate surface-bound functional groups on the nanotubes end.<sup>84,85</sup> The most common starting functionalisation method engaged to functionalise CNTs with covalent functionalisation is by oxidation process, which results in the formation of carboxyl groups (–COOH) on the surface of nanotubes. Oxidation has become a must in functionalisation because it oxidatively introduces carboxyl groups which is useful for further modifications. Carboxyl groups enable covalent coupling of molecules through the creation of amide and ester bonds.<sup>81,86</sup> There are two common acid treatments used; one refluxes the nanotubes with a solution of nitric acid<sup>87</sup> and the other exposes the sample to a mixture of sulphuric acid/nitric acid (HNO<sub>3</sub>/H<sub>2</sub>SO<sub>4</sub>) (1 : 3 by volume) under high power sonication for a maximum of 6 hours.<sup>88</sup> Fig. 6 shows the covalent functionalisation of nanotubes through oxidation process using H<sub>2</sub>SO<sub>4</sub>/HNO<sub>3</sub>.<sup>89</sup> As a result, the functionalisation provides stable dispersions of CNTs in a range of polar solvents, including with water.<sup>90</sup> Besides that, the covalent attachments of functional groups modify the stacking and layering properties of CNTs by altering the hydrogen bonding through reduction of van der Waals interactions between the CNTs and strongly facilitates the separation of nanotube bundles into individual tubes.<sup>91</sup>

Despite the fact that the first oxidations were developed to open and filling CNTs, the carboxyl, hydroxyl, and carboxylate groups generated all through surface oxidation of these materials have demonstrated useful moieties to bond new reactive chains that improve solubility, processing, and compatibility with other materials, thus allow scientists to take advantage of CNTs properties. Due to the relevance of this type of functionalisation, next sections shall deal with the different studies related to chemical functionalisation, after oxidation, by using



Fig. 6 Functionalisation of CNT through the oxidation process using H<sub>2</sub>SO<sub>4</sub>/HNO<sub>3</sub>. Adapted from ref. 43, copyright 2015, Elsevier.



the OH pertained to  $-\text{COOH}$  groups generated during the oxidation process. The organic carboxyl groups formed on a nanotube surface localised at the defects in functionalised single-walled and multi-walled nanotubes and suitable reactive organic groups from other chemical chains are prone to react in this zone. However, in some cases, deterioration due to employment of concentrated inorganic acids combined with high power sonication are responsible for creating a large number of defects on the CNTs sidewalls, and in some extreme cases, CNTs are fragmented into smaller pieces. These damages result in severe deterioration of mechanical, electrical, and thermal properties of CNTs.<sup>65</sup> This route greatly enhances the solubility of CNTs in common solvents and helps in dispersing CNTs in many polymer matrices. In addition to assisting in debundling, these treatments also significantly improve phase adhesion with the host matrix, thus help in processing of the polymer/CNT interface.

Goyanes *et al.* (2006) studied the effect of acid treatment and ultrasonication on MWCNTs using nitric acid with a mixture of  $\text{HNO}_3$  and  $\text{H}_2\text{SO}_4$  (1 : 3 by volume).<sup>92</sup> The sample was

ultrasonicated using ultrasonic bath (Selecta Ultrasons-H model, which has a nominal frequency of 40 kHz with power of 950 W). The preset time of sonication varied from 2, 4, and 6 hours. The result showed that the treatments with  $\text{HNO}_3$  and mixture of  $\text{HNO}_3$  and  $\text{H}_2\text{SO}_4$  (1 : 3 by volume), which were applied for a short period of time, did not show significant effect on the side walls of MWCNTs. An additional peak was observed at  $1200\text{ cm}^{-1}$  in the FTIR spectrum when the MWCNTs were treated with the acid mixture under ultrasonic vibration for 2 h, but their UV/Vis spectrum did not change significantly. These results indicate that new C–O groups appeared in the open ends of the nanotubes without modifying the structure of the sidewalls. Longer reaction time with the acid mixture treatment began to destroy the sidewalls of the nanotubes, as showed by the UV/Vis spectra. Finally, a longer treatment time of 6 hours completed the destruction of the nanotube sidewalls and shorter nanotubes were observed under atomic force microscopy (AFM), as shown in Fig. 7(a–e). The UV/Vis spectra of all samples are shown in Fig. 7(f).

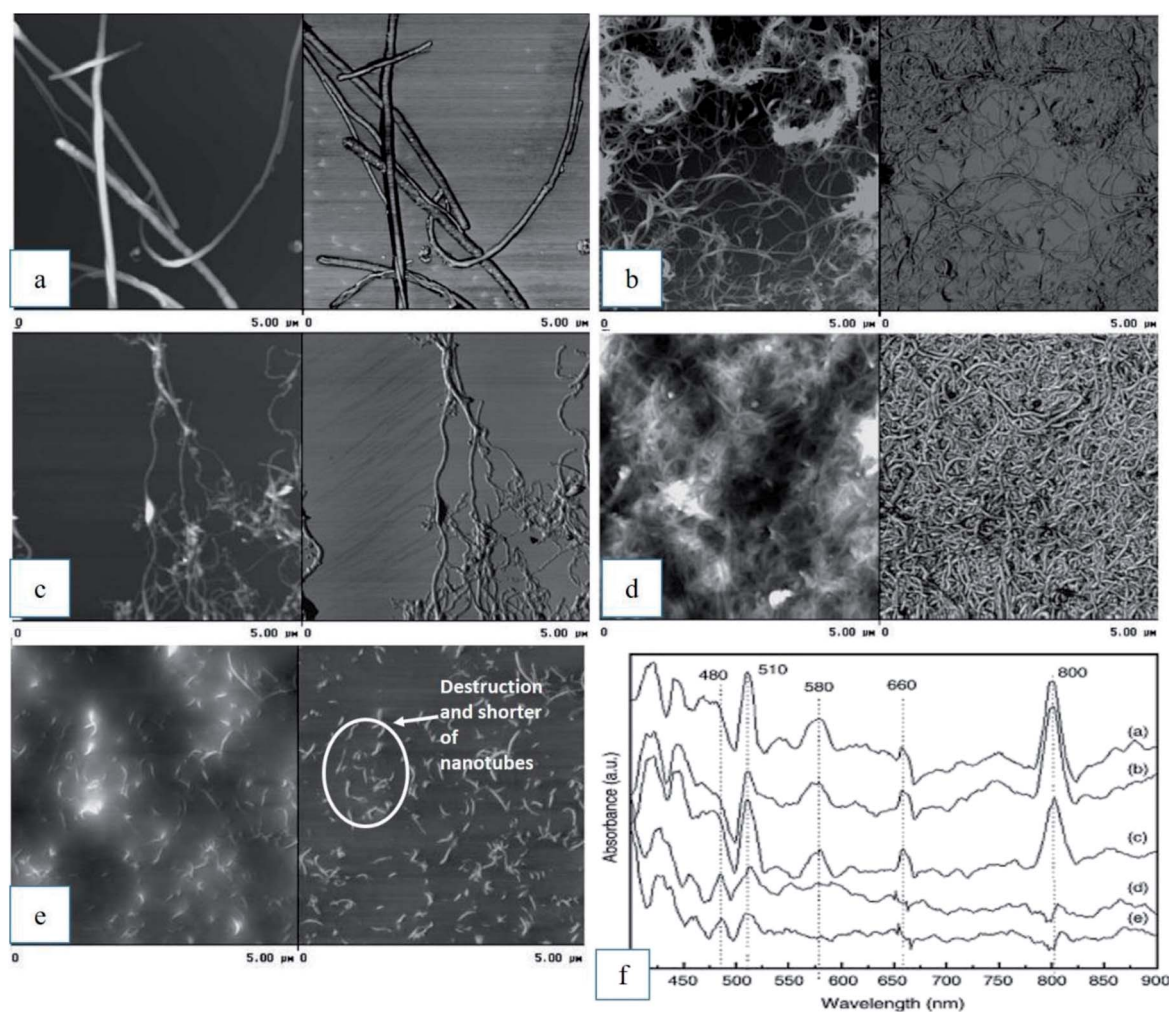


Fig. 7 AFM image (a) as-received MWCNTs and the effect of the oxidation process after: (b)  $\text{HNO}_3$  treatment; (c)  $\text{HNO}_3/\text{H}_2\text{SO}_4$  2 hour, (d)  $\text{HNO}_3/\text{H}_2\text{SO}_4$  4 hour, (e)  $\text{HNO}_3/\text{H}_2\text{SO}_4$  6 hour, and (f) UV/Vis spectra for sample (a) to (e). Reproduced with permission from ref. 92, copyright 2011, *Diamond and Related Materials*.





Chen *et al.* (1998) showed that the oxidation process for SWCNTs involved extensive ultrasonic treatment in a mixture of  $\text{HNO}_3/\text{H}_2\text{SO}_4$  (1 : 3 by volume) that led to the opening of the nanotube caps and the formation of holes in the sidewalls. The final products were fragments of nanotube with lengths of 100 nm to 300 nm, while the ends and sidewalls were decorated with a high density of various oxygen containing groups (mainly

carboxyl groups). However, under less vigorous conditions, such as refluxing in nitric acid, the shortening of the nanotubes can be minimised. Chemical modification was limited mostly to the opening of the nanotube caps and to the formation of functional groups at defect sites along the sidewalls.<sup>93</sup> Therefore, nanotubes functionalised in this manner basically retain their pristine electronic and mechanical properties.<sup>94</sup> As a result

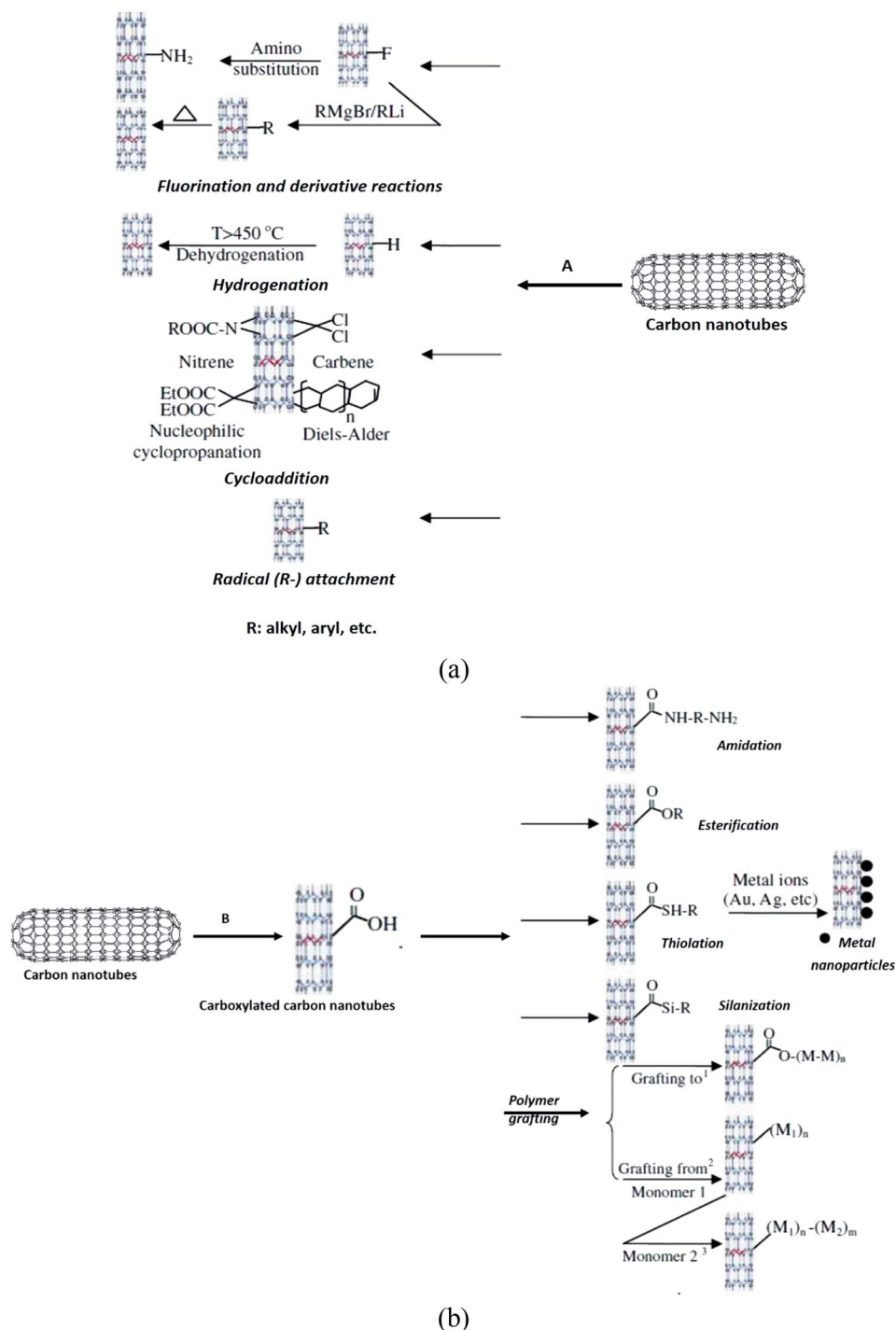


Fig. 8 The route of (a) covalent functionalisation of CNTs (A: direct sidewall functionalisation) and (b) (B: defect functionalisation). Reproduced with permission from ref. 65, copyright 2011, *Diamond and Related Materials*.





of the presence of fullerene-like end-caps which are sensitive to oxidation, the oxidation of CNTs may be readily performed to create oxidised CNTs.<sup>95,96</sup>

High chemical reactivity, such as fluorination of CNTs, has become popular for initial investigation of covalent functionalisation because the CNTs sidewalls were expected to be inert.<sup>97,98</sup> The fluorinated CNTs have C–F bonds that are weaker than those in alkyl fluorides,<sup>99</sup> thus providing substitution sites for additional functionalisation.<sup>100</sup> Besides sidewall fluorination of CNTs, other similar methods including cycloaddition, such as Diels–Alder reaction, carbene and nitrene addition,<sup>101,102</sup> chlorination,<sup>103</sup> bromination,<sup>104</sup> hydrogenation,<sup>105</sup> azomethine ylides,<sup>106</sup> have also been successfully functionalised and employed. All these methods can be regarded as derivatives of sidewall functionalisation of CNTs.

Furthermore, Ma *et al.* (2010) classified the functionalised CNT through carboxylation as defect functionalisation (Fig. 8).<sup>65</sup> This type of functionalisation has been discussed in Section 2. Referring to Fig. 8B, this process takes advantage of chemical transformation of defect sites on CNTs. Defect sites can be the open ends and/or holes in the sidewalls, pentagon or heptagon irregularities in the hexagon graphene framework. Oxygenated sites can also be considered as defects. Defects can be created on the sidewalls and at the open ends of CNTs by an oxidative process with strong acids such as HNO<sub>3</sub>, H<sub>2</sub>SO<sub>4</sub>, or a mixture of them,<sup>107</sup> or with strong oxidants such as KMnO<sub>4</sub>,<sup>108</sup> ozonolysis,<sup>109</sup> and reactive plasma.<sup>110</sup> The defects on CNTs created by oxidants are stabilised by bonding with carboxylic acid (–COOH) or hydroxyl (–OH) groups. Next, these functional groups have rich chemistry, thus the CNTs can be used as precursors for further chemical reactions, such as silanation,<sup>111,112</sup> polymer grafting,<sup>113</sup> esterification,<sup>114</sup> thiolation,<sup>115</sup> alkylation and arylation,<sup>116,117</sup> and even can be tagged with metal coordination compounds.<sup>118</sup> CNTs functionalised in this way are soluble in many organic solvents because the nature of CNTs is changed from hydrophobic to hydrophilic due to the attachment of polar groups. Chan *et al.* functionalised SWCNT with zwitterionic functional groups.<sup>119</sup> The functionalisation comprised of two steps. In the first step, SWCNT–COOH was reacted with thionyl chloride (SOCl<sub>2</sub>) to produce acetylated SWCNT. In the second step, the acetylated SWCNT underwent esterification using 3-dimethylamino-1-propanol, (CH<sub>3</sub>)<sub>2</sub>N–CC<sub>3</sub>H<sub>6</sub>–OH. As a result, the functionalised SWCNT has attached positive (tertiary amine group) and negative charges (carboxylated group).

Besides the attachment of carboxylic, hydroxyl, polymer, and other hydrophilic groups, attachment of inorganic compounds such as TiO<sub>2</sub> and Fe<sub>3</sub>O<sub>4</sub> on CNTs have been reported for electromagnetic and microwave absorption purposes.<sup>120,121</sup> Vatanpour *et al.* (2012) prepared MWCNT–TiO<sub>2</sub> *via* precipitation of TiCl<sub>4</sub> precursor on acid-treated MWCNT.<sup>122</sup> The acid treated MWCNT was functionalised with monohydrate citric acid. The synthesis of MWCNT–poly citric was aimed to get a better deposition of TiO<sub>2</sub> on the CNT. Next, TiO<sub>2</sub> nanoparticles were coated on MWCNT–poly citric acid by dispersing both functionalised CNT and TiCl<sub>4</sub> (as TiO<sub>2</sub> precursor) into a 1 M HCl solution at ambient temperature. Poly citric acid was then removed and the TiO<sub>2</sub> deposit was produced as the end-

product. Based on Wang *et al.* (2016), MWCNT/Fe<sub>3</sub>O<sub>4</sub> was prepared using a hydro-thermal method.<sup>123</sup> Prior to Fe<sub>3</sub>O<sub>4</sub> attachment, the CNT was acid-treated with an acid mixture of H<sub>2</sub>SO<sub>4</sub>/HNO<sub>3</sub> (3/1) for 4 h at 65 °C. The acid treated MWCNT was then mixed with FeCl<sub>3</sub> and FeSO<sub>4</sub> (molar ratio 2 : 1), and then ultrasonicated. The mixture was then stirred at 50 °C for 0.5 h and further stirred at 65 °C for 1 h at pH 12. The MWCNT/Fe<sub>3</sub>O<sub>4</sub> was obtained as precipitate and the hybrids improved the hydrophilicity of membrane surface, applied in trapping pollutants in membrane filtration.

The covalent functionalisation was widely used in CNTs application *via* acid treatment, carboxylation and fluorination methods. Based on the aforementioned studies, the covalent modification towards CNT composites produced high stability functionalisation. This mechanism led to efficient load transfer from the polymer/CNT matrix through covalent bonding. In addition, the covalent functionalisation severely altered the inherent properties of the CNTs; changed the electrical conductivity and thermal properties, and in some cases, shortened the length of nanotubes. Some CNT applications are incompatible with covalent modification, thus non-covalent functionalisation is preferred.

### 3. Non-covalent functionalisation of CNTs

Non-covalent functionalisation is a synonym interaction between CNTs and the interest conductive polymer. Referring to Bose *et al.* (2010), non-covalent functionalisation is an efficient alternative to tailor the CNT and polymer interface and yet preserving the reliability of the tubes.<sup>53</sup> This route is particularly attractive because of the possibility of adsorbing various groups of ordered architectures on the CNT surface without disturbing the extended p-conjugation of the nanotubes. In the last few years, non-covalent surface treatment has received lots of attention and various strategies have been proposed for the debundling of CNTs in the presence of a modifier. These approaches have been addressed in connection with surface coating/wrapping of low molecular weight surfactants (anionic/cationic),<sup>124,125</sup> polymers,<sup>126</sup> liquid crystalline p-conjugated oligomers,<sup>127</sup> and amphiphilic cationic polymer molecules.<sup>128</sup>

Non-covalent functionalisation is realised *via* enthalpy-driven interactions, such as π–π, CH–π, and NH–π, between the CNT surface and the dispersants and/or entropy-driven interaction; *i.e.* hydrophobic interaction using surfactants.<sup>129</sup> In the case of the surfactant dispersion, sodium dodecyl sulfate (SDS),<sup>130</sup> sodium dodecyl benzene sulfonate (SDBS),<sup>131</sup> sodium cholate (SC),<sup>132</sup> cetyltrimethylammonium bromide (CTAB),<sup>133</sup> Brij, Tween, and Triton X<sup>134</sup> have typically been used due to their availability and low cost.<sup>135</sup> The non-covalently surrounded polymers remained even after the washing process, such as filtration, to provide ‘polymer-wrapped CNTs’. In some applications, such wrapped dispersants act as a contaminant but in some cases, the wrapped CNTs synergistically improve the performance of the CNTs if the polymers are strategically designed and positioned.



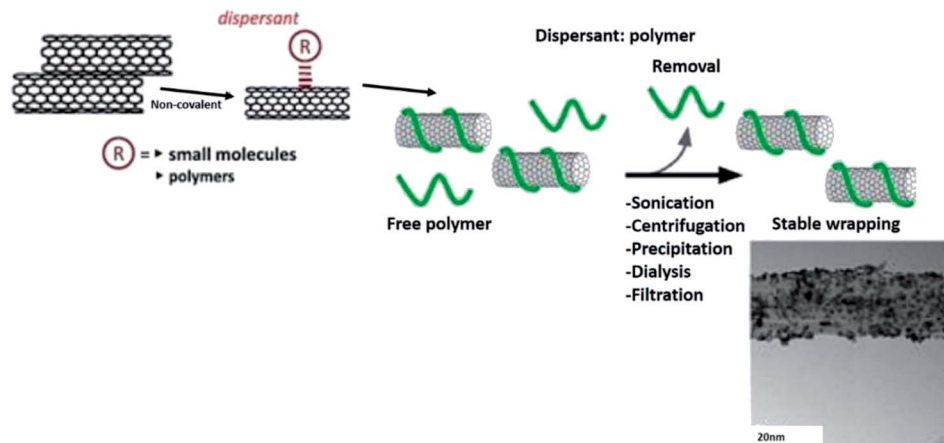


Fig. 9 Non-covalent functionalisation routes. Adapted from ref. 129, copyright 2015, Elsevier. And adapted from ref. 136, copyright 2015, Elsevier.

From numerous analytical models, it is quite evident that the percolation threshold has an intimate relationship with  $L/D$  of CNTs. Therefore, it can be stated that any types of pre-treatments that affect  $L/D$  of CNT would eventually influence the percolation thresholds in the composites. The 'effective  $L/D$ ' (of disentangled CNT) seems to be important in governing the percolation thresholds in the composites and the can be manipulated by various pre-treatments. The chemical functionalisation of CNTs adversely affects effective  $L/D$  due to the involvement of severe chemical conditions. In contrast, non-covalent routes enable significant exfoliation of CNTs mediated by the local environment of various modifiers and increase the effective  $L/D$ . Different pre-treatments involve different levels of interactions between molecules and the matrix, and greatly influence charge transport mechanisms in the composites.<sup>53</sup> Fig. 9 shows a schematic diagram of the non-covalent functionalisation routes of polymer towards CNTs.<sup>129,136</sup>

Due to the tailorable design of the polymers and the improvement of composites inherent properties, the concept of non-covalent functionalisation has recently been widely utilised and renowned. Compared to covalent functionalisation, this modification produces lower stability of functionalisation and ineffective polymer reinforcement due to the absence of covalent bonding between CNTs and polymer. Yet, non-covalent modification does not destroy the conjugated system of the CNTs side-walls and end-cap. Therefore, it does not affect the final structural properties of the material. Next, conjugated polymers wrapped meritoriously *via* non-covalent functionalisation of CNTs are due to  $\pi$ - $\pi$  stacking and van der Waals interactions between the polymer chains comprising of aromatic rings and the exteriors of CNTs. Non-covalent functionalisation is an alternative method of improving the interfacial properties of nanotubes.

## 4. Fabrication method of CNTs/nanocomposite

A variety of synthesis methods have been reported in order to incorporate CNTs into various polymeric interests. The main

motive is to prevent the agglomeration of CNTs and realise their uniformity dispersion inside polymer matrix. There is no single method to achieve perfect dispersion of different CNTs in different types of polymer matrices, which is universally applicable to all situations. Many factors need to be considered when selecting a proper technique for CNT dispersion, such as physical states of the polymer (solid or liquid) and chemical (thermoplastic or thermoset), dimensions and content of CNTs to be introduced, availability of techniques and fabrication processes, ease of its synthesis from suitable monomer, desired performance indices of composites and cost constraints, and the parameter of the solvent used. This section briefly describes the important processing methods for synthesis of CNT-based polymer nanocomposites.

### 4.1 Solution mixing

Solution mixing is the most common method for the fabrication of CNT/polymer nanocomposites because it is amenable to small sample sizes, and is one of the simplest fabrication methods for surface coating or making thin films.<sup>137</sup> Typically, solution mixing involves three major steps: dispersion of CNTs in a suitable solvent by mechanical mixing, magnetic agitation or sonication. The solvent can also dissolve polymer resins. Subsequently, the dispersed CNTs are mixed with polymer matrix at room or elevated temperatures. The nanocomposite is finally obtained by precipitating or casting the mixture. However, an often encountered limitation in solution mixing is the slow evaporation of solvent that provides sufficient time for CNTs re-agglomeration and differential settling, resulting in homogenous CNTs dispersion in matrix (*e.g.* CNTs content is lowest at the casted film/sheet's surface, and shows a uniform/random gradient across the thickness and maximum at both surfaces due to the extensive tube settling) and observation of non-uniform and inferior properties.<sup>138</sup> The solvent evaporation rate-related limitations can be resolved by gently pouring CNT/polymer nanocomposite dispersion on a rotating substrate (spin coating)<sup>139</sup> or over a heated substrate (drop-casting).<sup>140</sup> However, use of spin coating is limited only to thin films (few



nanometres thick) which cannot be peeled off from the substrate, whereas drop casting has issues in terms of uniform drying across thickness and high possibility of void formation. Another versatile method exploits coagulation<sup>141</sup> of CNT/polymer dispersion by pouring into an excess of non-solvent, thereby achieving rapid precipitation of polymer chains which immediately entrap CNTs (without providing sufficient time for CNTs diffusion and settling). Nevertheless, solution processing is still widely used and is one of the important steps in the processing of thermosetting matrices-based nanocomposites.

#### 4.2 Melt blending

Melt blending is another commonly used method to fabricate CNT/thermoplastic polymer nanocomposites. Thermoplastic polymers, such as polyethylene,<sup>142</sup> polypropylene,<sup>143</sup> polystyrene,<sup>144</sup> and other thermoplastic polymer can be processed as matrix materials in this method. The major advantage of this method is that no solvent is employed to disperse CNTs. Melt blending uses high temperature and high shear force to disperse CNTs in a polymer matrix and is most compatible with current industrial practices. Special equipment, such as mini-extruder and injection machine, which are capable of being operated at an elevated temperature and generate high shear forces, are employed to disperse CNTs. Melt blending or variants of this technique are frequently used to produce CNT/polymer composite fibres. Compared with the solution mixing methods, this technique is generally considered less effective to disperse CNTs in polymers, and its application is also limited to low filler concentrations in thermoplastic matrices.<sup>145</sup>

#### 4.3 *In situ* polymerisation

*In situ* polymerisation is an efficient method to obtain uniform dispersion of CNTs in a thermosetting polymer (Fig. 10). In this

method, CNTs are mixed with monomers, either in the presence or absence of a solvent, and then these monomers are polymerised *via* addition or condensation reactions with a hardener or curing agents at an elevated temperature. One of the major advantages of this method is that covalent bonding can be formed between the functionalised CNTs and polymer matrix, resulting in much improved mechanical properties of composites through strong interfacial bonds. This method often gives better filler dispersion, especially at higher filler contents than melt mixing, and in the case of *in situ* polymerisation, it is possible to separate aggregated nanotubes with low energy input in a solvent with low viscosity like toluene in pre-treatment.<sup>146</sup> This approach uses a wet chemical online-filled method to prepare ferrite-filled MWCNTs and *in situ* chemical synthesis of chitosan-decorated ferrite-filled MWCNTs/polythiophene composites. The decoration of chitosan onto the surface of the ferrite-filled MWCNTs improves the dispersion of the ferrite-filled MWCNTs in the matrix of polythiophene and reduces the agglomeration of the ferrite-filled MWCNTs. Furthermore, this method is applicable for the preparation of other MWCNT-magnetic composites such as surfactant-decorated  $M_xFe_{2-x}O_4$ -filled MWCNTs/conductive polymer composites for use in the electromagnetic devices.<sup>147</sup>

#### 4.4 Latex technology

A relatively new approach to incorporate CNTs into a polymer matrix is based on the use of latex technology. Latex is a colloidal dispersion of discrete polymer particles, usually in an aqueous medium. By using this technology, it is possible to disperse single and multi-walled CNTs in most polymers that are produced by emulsion polymerisation, or that can be brought into the form of an emulsion. Contrary to the *in situ* polymerisation system, the addition of CNTs in this technique

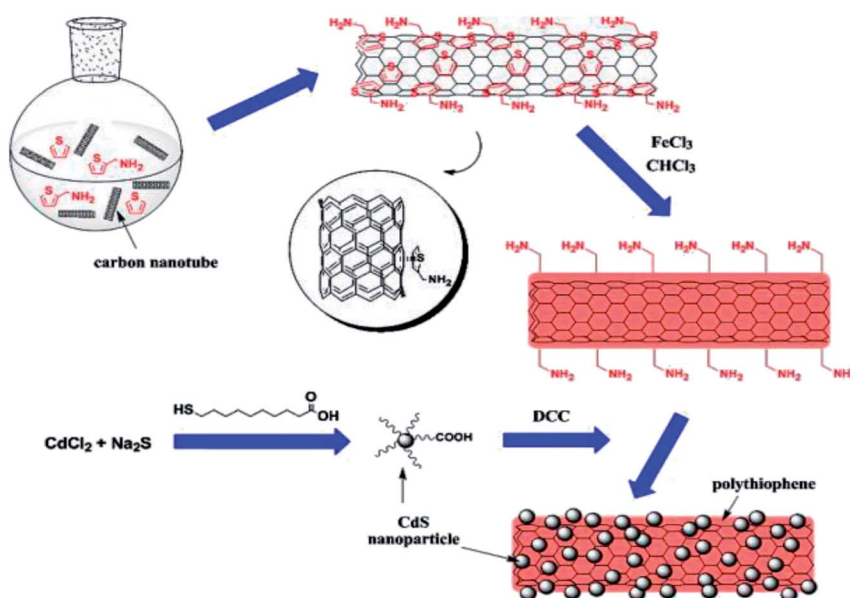


Fig. 10 Schematic diagram of decorating MWCNTs with CdS NPs with *in situ* polymerised PTh acting as an inter-linker. Reproduced with permission from ref. 148, copyright 2015, Elsevier.



takes place after the polymer has been synthesised. The first step of the process consists of exfoliation (for SWCNT bundles) or dispersion/stabilisation (for MWCNT entanglements) of CNTs in an aqueous surfactant solution. This is followed by mixing the stable dispersion of surfactant-treated CNTs with polymer latex. After freeze-drying and subsequent melt-processing, a nanocomposite consisting of dispersed CNTs in a polymer matrix is obtained. The advantages of this technique are obvious; the whole process is easy (because it basically consists of a simple mixing of two aqueous components), versatile, reproducible, and reliable, and allows incorporation of individual CNTs into a highly viscous polymer matrix. The solvent used for CNT dispersion is water, thus the process is safe, environmentally friendly, and low-cost. Nowadays, polymer latex is industrially produced in a large scale. Fig. 11 shows the preparation of MWCNTs efficiently dispersed in natural rubber (NR)-latex with the aid of hyper branched tri-chain sulphosuccinate anionic surfactants, specifically sodium 1,4-bis(neopentyloxy)-3-(neopentyloxycarbonyl)-1,4-dioxobutane-2-sulphonate (TC14). The results revealed that the introduction of a third chain with terminal methyl groups on the surfactant chains profoundly influences the homogenisation of MWCNTs in NR-latex matrices. Interestingly, the results are consistent with the results of surface tension studies,<sup>149</sup> where the introduction of a third chain with a highly methylated group lowers the surface energy, resulting in efficient partitioning at the MWCNTs/NR-latex interface.<sup>150</sup> Table 2 tabulates the summary of the fabrication methods of CNT/nanocomposites.

#### 4.5 Other methods

To obtain CNT/polymer nanocomposites with very high CNT content or for some specific applications, new methods have been developed in recent years. The new methods include densification, sol-gel method, spinning of coagulant, layer-by-layer deposition, and pulverisation.

## 5. Functionalised CNTs in chemical sensor

Chemical sensors are attracting tremendous interest because of their widespread applications in industry, environmental monitoring, space exploration, biomedicine, and pharmaceuticals. Gas sensors with high sensitivity and selectivity are required for leakage detections of explosive gases such as hydrogen, and for real-time detections of toxic or pathogenic gases in industries. There is also a strong demand for the ability to monitor and control the environment, especially with the increasing concerns on global warming.<sup>151–153</sup> There are several types of sensors intended for various applications that include electrochemical sensors, biosensors, surface acoustic wave sensors, immunosensors, and chemiresistive sensors. However, a leading candidate is the chemiresistor, which is chemical sensor based on the simple change in resistance in response to the binding of analytes. Advantages of chemiresistors include low power consumption and the ease of high precision resistance measurements.<sup>154</sup>

This review section discusses the application of functionalised CNTs in chemiresistive sensors. Chemiresistive sensor is one of the best transduction units, attributing to its simplicity, rapid response, and low-cost procurement. These are also the reasons why most commercialised gas sensors are fabricated into chemiresistive sensors.<sup>155</sup> A chemiresistive sensor translates chemical information *via* the changing in two-point contact electrical resistance.<sup>156</sup> Electrical resistance is a simple electrical signal to be analysed and requires only minimum supportive electronics for building deployable, compact, and self-contained systems. For the case of conducting polymer, this operation mode is greatly alterable upon nano-structuring. The resulting sensors exploit composition and structure dependent charge transport as well as adsorption, in order to fine-tune the gas sensor performance.<sup>157</sup> In chemiresistive sensors, an active



Fig. 11 Schematic diagram of the latex technology of MWCNTs dispersed in NR latex. Reproduced with permission from ref. 150, copyright 2015, Elsevier.





Table 2 Summary of the fabrication methods of CNT/nanocomposites

Specification	Solution mixing	Melt binding	<i>In situ</i> polymerisation	Latex technology
Mechanism	(1) Dispersion of CNTs in solvent (magnetic stirring, reflux, and ultrasonication), (2) mixing with polymer, (3) recovery of the nanocomposites (casting a film)	Involves the melting of polymer pellets into viscous liquid with high shear forces application	Involves mixing of nanofiller with monomers in a solvent, followed by <i>in situ</i> polymerisation	The CNT dispersion is mixed with a given polymer latex to form homogenous CNT/latex dispersion
Advantages	(1) Wider applicability, (2) better dispersion, (3) rigorous mixing in solvent	(4) Wide applicability, (5) good dispersion, (6) low cost, (7) simplicity to facilitate large scale production	(8) Widest applicability, (9) best dispersion, (10) enables grafting of polymer macromolecules onto the wall of CNTs, (11) allows preparation of nanocomposites with high CNT loading, (12) very good miscibility with polymer matrix	(14) Possible in disperse CNTs in polymers produced by emulsion polymerisation, (15) facile process, (16) reproducible, and reliable, (17) allows incorporation of individual CNTs into a highly viscous polymer matrix
Disadvantages	Slow evaporation lead to CNTs aggregation, (1) inapplicable for industrial scale processes, (2) low stability, (3) Residual solution	(4) High shear force and temperature can deteriorate nanocomposite and polymer intrinsic properties, (5) poor dispersion, (6) large residual stress, (7) low interfacial bonding strength	(9) Involve complex procedures and processing steps, (10) requires expensive reactants, (11) residual monomer, (12) large residual stress, (13) matrix strength decline	(14) Mechanical properties of the material were not significantly improved

layer is usually deposited over an array of electrodes to measure the electrical resistance change in the presence of target analytes. The primary charge carrier and type of gas interacting with the active layer induce the change of sensor's resistance upon gas exposure.<sup>158,159</sup>

Several materials have been utilised and added as fillers in gas sensors, including metal oxides, organic semiconductors, and carbon nanotubes.<sup>160</sup> Metal oxides are the most widely used materials for chemiresistors.<sup>161</sup> Even with their sensitivity, the applications of these materials have been limited by high power consumption and poor selectivity. Organic semiconductors, especially conjugated polymers, have long been considered as chemiresistor materials.<sup>162</sup> The integration of molecular recognition into their structures is attractive. However, these materials are limited by electrostatic/dielectric interferences and fragile organic-metal interfaces. CNT field effect transistors have been studied as chemical and biological sensors.<sup>163–165</sup> These devices are sensitive because their resistance can change drastically in the presence of analytes *via* charge transfer (doping), carrier pinning, and/or modification of the Schottky barrier at the nanotube/metal contact. Among existing sensor materials of metal oxides, organic semiconductors, and CNTs, the latter are particularly intriguing because of its unique properties such as large surface area, good environment stability, and excellent mechanical properties.<sup>166,167</sup>

Theoretically, the carbon atoms in a carbon nanotube are surface atoms, which makes them optimally suited for components of chemical sensors. Hence, it is not surprising that gas sensors made from individual nanotubes show good sensitivity and exhibit fast response and substantially higher

sensitivity than that of existing solid-state sensors at room temperature upon the exposure to gaseous molecules such as NO<sub>2</sub> or NH<sub>3</sub>,<sup>168,169</sup> in comparison to commercially available classical semiconductor sensors, which in general operate above 200 °C.<sup>170</sup> However, a necessary prerequisite is that the molecules to be detected must have a distinct electron donating or accepting ability, for example, NH<sub>3</sub> as a donor and NO<sub>2</sub> as an acceptor.

It has been reported that CNTs are very sensitive to the surrounding environment. The presence of O<sub>2</sub>, NH<sub>3</sub>, NO<sub>2</sub> gases and many other molecules can either donate or accept electrons, resulting in an alteration of the overall conductivity.<sup>171,172</sup> This is because the adsorption of these molecules on the nanotubes is associated with a partial charge transfer, which alters the charge-carrier concentration, or alternatively, the adsorbed molecules may affect the potential barriers present at the tube-electrode contacts. In any circumstance, the resulting change in the electrical resistance of the individual nanotube is utilised as a sensor signal. However, for the detection of molecules that are only weakly adsorbed (*e.g.*, CO and H), the change in resistance is often too small. A possible method to overcome this drawback is by the functionalisation of the side wall of CNT with a conductive polymer.

Since the most common gas sensing principle is the adsorption and desorption of gas molecules on sensing materials, it is quite understandable that by increasing the contact interfaces between the analytes and sensing materials, the sensitivity can be significantly enhanced. Recent development in nanotechnology has created huge potential to build highly sensitive, low cost, portable sensors with low power



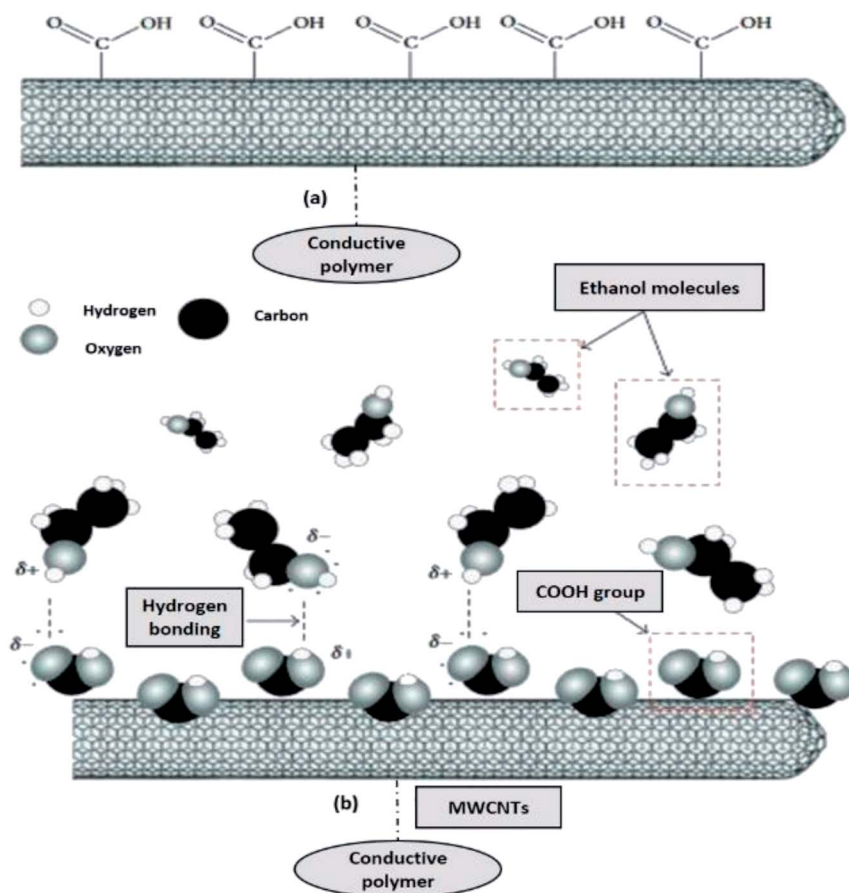


Fig. 12 (a) Schematic diagram of carboxylated functionalised of MWCNTs, and (b) proposed mechanism for ethanol (alcohol) vapour detection using conductive polymer–MWCNTs–OOH sensors. Adapted from ref. 176, copyright 2015, Elsevier.

consumption. The extremely high surface-to-volume ratio and hollow structure of nanomaterials is ideal for adsorption and storage of gas molecules. Therefore, gas sensors based on nanomaterials with conductive polymer, such as CNTs, nanowires, nanofibers, and nanoparticles, have been investigated widely.<sup>173–175</sup> Fig. 12 shows the schematic diagram of chemically conductive polymer-functionalised MWCNTs, which contain COOH groups attached along the sidewall of the MWCNTs and (b) the proposed mechanism for ethanol (alcohol) vapour detection using MWCNTs–OOH sensors, where the COOH groups tend to react with the ethanol molecules at room temperature.<sup>176,177</sup>

Many different types of organic materials have been used for gas sensing. The simplest organic compounds that can be electrically conductive are polymers, based on carbon and hydrogen.<sup>178</sup> Organic conducting polymers including polypyrrole (PPy),<sup>179</sup> polyaniline (PANI),<sup>180</sup> polythiophene (PTh),<sup>181</sup> poly(3,4-ethylenedioxythiophene) (PEDOT),<sup>182</sup> and polyacetylene (PA)<sup>183</sup> are examples of materials for fabricating gas sensors. Organic polymers are one of the principal materials applied in gas sensing systems. Some conducting polymers can behave like semiconductors due to their heterocyclic compounds which display physicochemical characteristics. As a result, reversible changes in the sensing layer's conductivity

can be detected upon polar chemicals' adsorption on the surfaces at room temperature.<sup>184</sup> This effect is believed to be caused by the charge transfer between gas molecules and the polymer or the polymer film's swelling.<sup>185</sup> This sensing response has intensively increased motivation to develop high sensitive and selective chemical sensors by tailoring the compounds of different organic polymers with functionalised CNTs.

Due to adsorption of interested analytes, there are volumetric changes of the matrix polymer. This leads to a distinct change in percolation-type conductivity around a critical composition of the material, which is known as "percolation threshold". Generally, the percolation threshold is dependent on the shape of the conducting particle. Conductive polymer consisting of particles with higher aspect ratio shows lower threshold and higher sensitivity.<sup>186</sup> CNTs, with almost one-dimensional thread-like structure and good conductivity, are ideal as the dispersed particles in this conducting particles-insulating matrix composition for gas sensing systems. Therefore, CNTs/conductive polymer have been intensively studied for gas sensors.<sup>187–190</sup>

The nanocomposite of PPy and carboxylated multi-walled carbon nanotubes (MWCNT–COOH) was synthesised by *in situ* chemical oxidative polymerisation method using HCl as a dopant and ammonium persulphate (APS) as an oxidant for



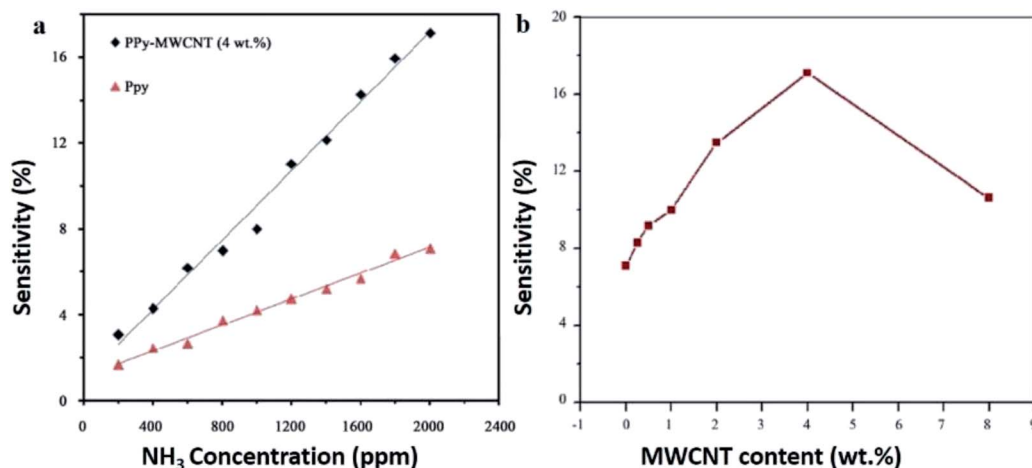


Fig. 13 Sensitivity of PPy/MWCNT with (a) different NH<sub>3</sub> concentration and (b) different MWCNT loadings towards the NH<sub>3</sub> at 2000 ppm. Reproduced from ref. 191, copyright 2015, Elsevier.

the detection of NH<sub>3</sub>.<sup>191</sup> The synergistic effects of the PPy-coated MWCNTs showed that the most sensitive PPy/MWCNT nanocomposites sensor towards NH<sub>3</sub> gas was obtained at 4 wt% MWCNT content and found to be stable in operation against the variation in operating temperature and humidity (Fig. 13). The increase in sensitivity with increase in MWCNT content is attributed to the increase in surface area of the composite material, providing more active sites for adsorption of NH<sub>3</sub> gas molecules. Thus increase in sensitivity and further increase in MWCNT content leads the nanocomposite electrically shorted, thereby increasing the percolation effect by highly conductive carbon nanotubes. Besides, increased sensitivity from 3.07% to 17.11% over 200 to 2000 ppm of NH<sub>3</sub> concentration is because the sensitivity of sensor depends on the removal of adsorbed oxygen molecules by reaction of target analyte and generation of electrons. For smaller gas concentration exposed on the fixed surface area of sensor, lower surface reaction occurred due to

lower exposure of analyte. On the other hand, an increase in gas concentration raises the surface reaction due to larger surface exposure. Fig. 14 shows the comparison of gas sensing sensitivity of PPy/MWCNT (4 wt%) sensor towards 2000 ppm NH<sub>3</sub> with other analytes.

Low-cost, conductive Pap@CNT-NH<sub>2</sub>@PPy (conductive paper strip) composites were prepared through sonochemical polymerisation of pyrrole in the presence of oxidising agent and tosylate co-dopant (TS) on cellulosic paper strips decorated with aminophenyl-modified (MWCNT-NH<sub>2</sub>).<sup>175</sup> The Pap@CNT-NH<sub>2</sub>@PPy end materials served as chemiresistive NH<sub>3</sub> sensors exhibited an outstanding response of 525% to 0.1 ppm level of NH<sub>3</sub> at room temperature with good stability for a long period of time and remained the same at different times, resulting in highly reproducible sensing characteristics. Comparative gas sensing properties analysis of the nanocomposite-based gas sensors synthesised with different ratio molar CNT/amine revealed excellent sensor performance for Pap@CNT-N1/1@PPy nanocomposite in the concentration range of 0.005 to 0.05 ppm of NH<sub>3</sub> with high sensitivity and low LOD of 0.04 ppb. An increase in the electrical resistance of CNT@PPy sensor was observed when it was exposed to NH<sub>3</sub> gas. This attributed to the charge transfer mechanism between NH<sub>3</sub> and CNT@PPy surface. As a matter of fact, upon the interaction of NH<sub>3</sub> with PPy, the polymer loses its electron and this electron transfer between PPy positive holes and NH<sub>3</sub> causes a depression in the charge-carrier concentration resulting in decreased overall conductivity. However, in air, the reverse reaction that NH<sub>4</sub><sup>+</sup> ion decomposes into ammonia takes place and changes the conductivity of PPy to higher values. The mechanism of the PPy-NH<sub>3</sub> interaction is as follow:



Fig. 14 Gas sensing sensitivity of PPy/MWCNT (4 wt%) sensor towards 2000 ppm of NH<sub>3</sub>. Reproduced from ref. 191, copyright 2015, Elsevier.

Philip *et al.* (2003) fabricated a nanocomposite thin film of polymethylmethacrylate (PMMA) with MWCNTs and oxidation-modified MWCNTs (f-MWCNTs) for gas sensing purposes.<sup>192</sup> The



Table 3 Responsiveness of the nanocomposites

Vapours	Responsiveness ( <i>S</i> )	
	CNT/PMMA	f-CNT/PMMA
DCM	9.94	809
Chloroform	7.57	407
Acetone	6.35	84
Methanol	4.29	45
Ethyl acetate	2.23	30
Toluene	2.24	1.04

resistance changes of both nanocomposites were evaluated upon exposure to dichloromethane, chloroform, and acetone. Both the CNT/PMMA and the f-CNT/PMMA nanocomposites showed increasing resistance upon exposure to these vapours at room temperature. Table 3 indicates that the different nanocomposites have different responsiveness (*S*) or sensitivity towards the applied vapours. This behaviour was explained on the basis of volume expansion and polar interaction of the CNT surface with vapour molecules. The f-CNT/PMMA showed significant improvement on the sensor's behaviour including in

sensitivity and the response time and recovery, as shown in Fig. 15. This can be explained by the effects of oxidation on the electronic properties of CNTs. In non-functionalised CNT/PMMA composites, the dispersion of CNTs in the polymer matrix is not uniform. This means that there is only a small volume through which the nanotubes form a conducting path through the polymer matrix so that the increase in resistance due to swelling of the PMMA matrix is less. The responsiveness of the nanocomposites can be determined from equation

$$S = \frac{R - R_0}{R_0} \quad (1)$$

where  $R_0$  is the initial resistance and  $R$  is the maximum steady state resistance value.

The oxidation functionalisation of nanotubes built COOH and OH groups along the sidewall and the caps of the CNTs.<sup>193</sup> The created functional groups can physically interact through the PMMA, resulting in strong interfacial adhesion and better dispersion of f-CNTs in the polymer matrix. The volume of the conducting channel through the PMMA matrix is large so that a small swelling of the matrix can induce a large increase in resistance. This explains the large increase in response for f-CNT composite when exposed to dichloromethane,

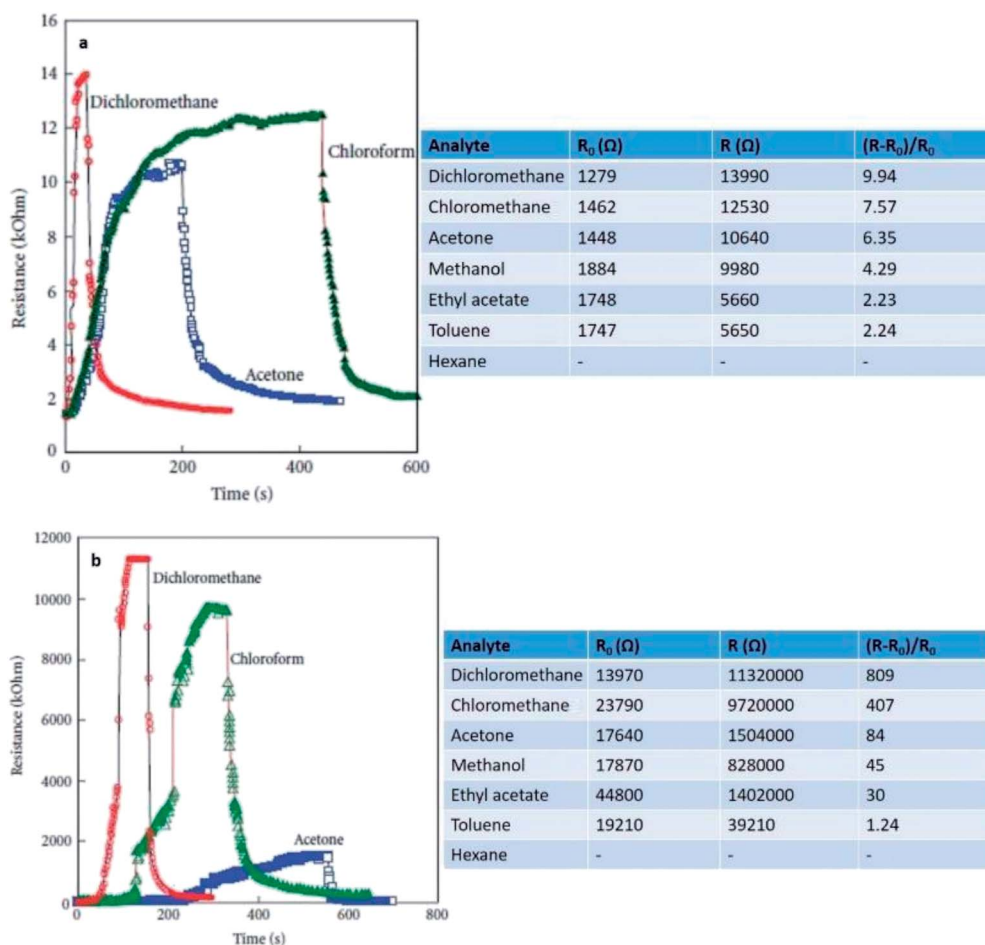


Fig. 15 (a) Response of the CNT/PMMA composite to analytes and sensor response, and (b) response of the f-CNT/PMMA composite to analytes and sensor response towards dichloromethane, chloroform and acetone vapours. Reproduced from ref. 194, copyright 2015, Elsevier.





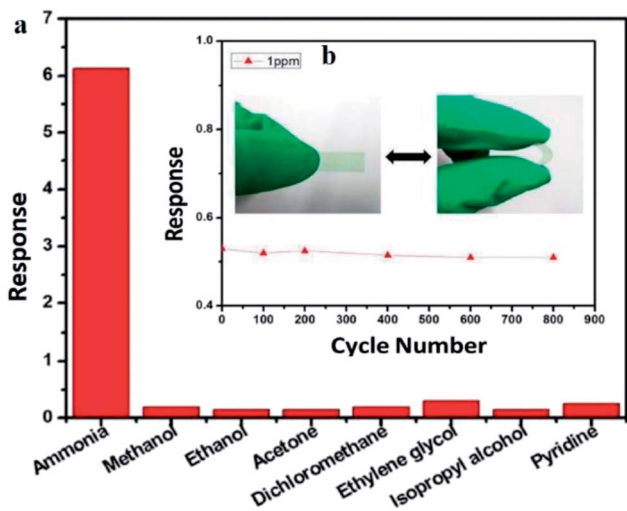


Fig. 16 (a) Selectively sensing response to 10 ppm of  $\text{NH}_3$  and other analytes for the PANI/MWCNT nanocomposite film and (b) gas sensing response of the PANI/MWCNT nanocomposite film in bending and extending states to 1 ppm of  $\text{NH}_3$ . Reproduced from ref. 198, copyright 2017, Elsevier.

chloroform, and acetone, which can swell the polymer matrix to a large extent. The polar groups on the nanotube surface also increased by adsorption of solvent molecules and give a better response. This is proved by the fact that polar solvents like methanol showed an improved response to f-CNT/PMMA composites even though they are not good solvents for PMMA.

Inspired by the enhanced gas-sensing performance of the one-dimensional hierarchical structure, one-dimensional hierarchical PANI/MWCNT were prepared.<sup>195</sup> The p-type PANI/MWCNT (p-PANI/MWCNT) and n-type PANI/MWCNT (n-PANI/MWCNT) showed higher sensitivity towards  $\text{NO}_2$  and  $\text{NH}_3$ , respectively, where the response times of p-PANI/CNT and n-PANI/CNT to 50 ppm of  $\text{NO}_2$  and  $\text{NH}_3$  were only 5.2 and 1.8 s, respectively. The estimated limit of detections (LOD) for  $\text{NO}_2$  and  $\text{NH}_3$  was as low as 16.7 and 6.4 ppb, respectively. After three



Fig. 18 Variation in sensor response toward  $\text{CHCl}_3$  vapour as a function of c-MWCNT concentration in PANI/c-MWCNT nanocomposite. Reproduced from ref. 199, copyright 2015, Elsevier.

months, the responses of p-PANI/CNT and n-PANI/CNT decreased by 19.1% and 11.3%, respectively. It was found that the one-dimensional hierarchical structures and deeper charge depletion layer enhanced by structural changes of PANI contributed to the sensitive and fast responses to  $\text{NO}_2$  and  $\text{NH}_3$ . This work also looks forward to the development prospects of cost effective and high-performance PANI/MWCNT-based sensors in the potentials of interface engineering in improving gas-sensing performance.

In addition, Zhang *et al.*<sup>195</sup> (2020) suggested that the high and fast response of the nanocomposites should be attributed to the following three factors; (1) for the hierarchical p-PANI/MWCNT, a large number of micropores exist in the conductive networks of hierarchical p-PANI/MWCNT arranged in disorder and the hierarchical structure provides a large number of passageways, which provide sufficient and fast channels for



Fig. 17 Suggested mechanism of  $\text{CHCl}_3$  molecules with PANI/c-MWCNT nanocomposite. Reproduced from ref. 199, copyright 2015, Elsevier.



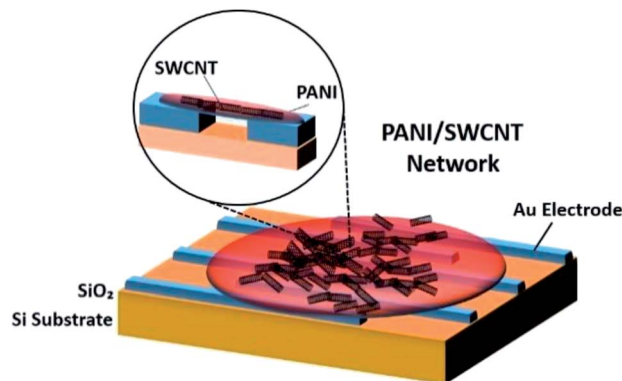


Fig. 19 Schematic diagram of PANI coated with SWCNT-COOH on interdigitated electrodes. Adapted from ref. 200, copyright 2015, Elsevier.

the diffusion. It is well known that gas-sensing process occurs mainly on the surface of sensing materials. Therefore, the effective exposure of sensing materials to the gas molecules largely determines the sensor's sensing performance. The high permeability of hierarchical p-PANI/MWCNT allows target gas molecules to rapidly contact with PANI fibres by rapid diffusion through the channels, hence shortening the response and recovery time, and enhancing the sensitivity. (2) Compared with PANI, MWCNTs demonstrate higher carrier mobility. Therefore, the carrier mobilities of PANI can be reinforced by constructing core-shell PANI/MWCNTs composites. The conjugated

interfaces between PANI and MWCNTs provide the percolation path with higher carrier mobility. Furthermore, when the target gas ( $\text{NO}_2$ ) is in contact with the p-PANI/MWCNTs, the process of charge transfers between the target gas and the hierarchical p-PANI/MWCNTs is accelerated due to the enhanced carrier mobility, *i.e.*, the response and recovery time are also shortened. (3) Due to electron-rich amino groups of PANI. For electron-deficient  $\text{NO}_2$ , these electron-rich amino groups of PANI act as baits to induce the oxidation of  $\text{NO}_2$  to be adsorbed on the surface of PANI, enhancing the sensitivity. Due to the uniform core-shell structure of n-PANI/MWCNT, many p-n heterojunctions are formed at the interface between n-type PANI and p-type MWCNTs. Therefore, the n-PANI/MWCNT not only have the above advantages of p-PANI/MWCNT, but also have a unique p-n heterojunction structure. The combination of electrons in n-type PANI and holes in p-type MWCNTs at the interface result in lower carrier concentration, enhancing the sensitivity of n-PANI/MWCNT.<sup>196,197</sup>

Another study on  $\text{NH}_3$  detection was done by Xue *et al.* (2017) using PANI/MWCNT.<sup>198</sup> The nanocomposites showed high sensitivity towards  $\text{NH}_3$  from 200 ppb to 50 ppm, fast response and recovery time with 85 s and 20 s, respectively at room-temperature operation without external aid, reliable flexibility and excellent selectivity to  $\text{NH}_3$  compared to other volatile organic compounds (Fig. 16). The excellent sensing performance is probably ascribed to the synergetic effects of PANI and MWCNT, the high surface area ( $54.187 \text{ m}^2 \text{ g}^{-1}$ ) of nanocomposite films, and effective network sensing channels. The

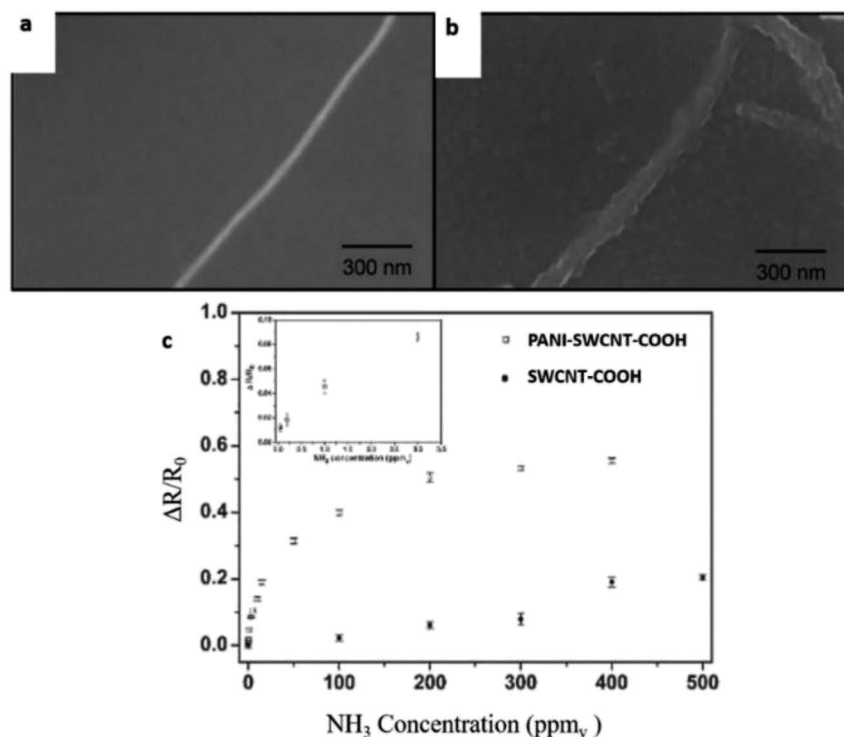


Fig. 20 (a) SEM images of a bare SWCNT before electropolymerisation, (b) SEM image of coated SWCNT-COOH after electropolymerisation, and (c)  $\text{NH}_3$  sensitivity of PANI-SWCNTs-COOH and unfunctionalised SWCNTs (SWCNT-COOH, without PANI). Reproduced from ref. 200, copyright 2015, Elsevier.





Fig. 21 The chemical structure of P3OT and P3CT, and their responses of the P3CT/SCNT, P3OT/CNT sensor, and the non-functionalised CNT sensor to 20 s vapour exposures of various compounds (1% of saturated vapour) and 32 ppb of NMPEA. Reproduced from ref. 201, copyright 2018, Elsevier.

film with simple preparation, high sensitivity, small size, and robust flexibility, could be implanted into electronic devices for potentially monitoring  $\text{NH}_3$  in anaerobic digestion in real-time for the high efficiency and better stability of anaerobic digestion for renewable energy sources. In short, electrons provided from the adsorbed  $\text{NH}_3$  molecules onto PANI transfer easily from PANI to MWCNT because of the lower conductivity of PANI and lower energy barrier between PANI and carbon nanomaterials, about 101 meV. Then, the electrons effectively transfer from MWCNT to the PANI fibre due to lower energy barrier and finally to the electrodes. Therefore, the sensing response was effectively improved in PANI/MWCNT nanocomposite network.

PANI nanocomposites doped with carboxylic acid functionalised multi-walled carbon nanotube (c-MWCNT) were synthesised by *in situ* chemical oxidation polymerisation of aniline monomer using ammonium persulfate in the presence of c-MWCNT.<sup>199</sup> The nanocomposites showed better response to chloroform ( $\text{CHCl}_3$ ) vapour as compared to pure PANI. Fig. 17 shows the suggested mechanism of  $\text{CHCl}_3$  molecules with PANI/c-MWCNT nanocomposite. For nanocomposite sensors, the sensing performances in terms of sensor response, response time, and reproducibility increased with increasing c-MWCNT concentration, up to 3 wt% (Fig. 18), while the response of the 2 wt% pristine MWCNT in the nanocomposite ( $S = 3.4$ ) was found to be ten times lower than that of the PANI/c-MWCNT nanocomposite (PC3) ( $S = 32.8$ ) at chloroform concentration of 250 ppm. This indicates good selectivity and response of PANI/c-MWCNT towards chloroform rather than pure PANI/MWCNT. Next, the decrease in DC electrical resistance of c-MWCNT-doped PANI nanocomposite upon exposure to chloromethane vapour indicates significant interactions between vapour molecules and conjugated PANI chains. Among the studied nanocomposite sensors, the highest sensing capability was observed for the sensor containing 3 wt% c-MWCNTs. The sensor response exhibited a good linear relationship with c-MWCNT concentration at all studied  $\text{CHCl}_3$  concentrations. The difference in response of the PANI/c-MWCNT sensor for different chlorinated methane vapours could be utilised for selective detection of the vapours.

Zhang *et al.* (2006) demonstrated a facile fabrication method to make chemical gas sensors using carboxylated SWCNT (SWCNT-COOH) with 80 to 90% purity and were electrochemically functionalised with PANI.<sup>200</sup> The potential advantage of the proposed method is to enable targeted functionalisation with different materials to allow for creation of high-density individually addressable nano sensor arrays. The PANI-SWNT-COOH network-based sensors were tested for on-line monitoring of ammonia gas. The results showed superior sensitivity of 2.44% response of  $\text{NH}_3$  (which is 60 times higher than intrinsic SWNT based sensors), a detection limit as low as 50 ppb<sub>v</sub>, and good reproducibility upon repeated exposure to 10 ppm<sub>v</sub>  $\text{NH}_3$ . Higher sensitivities were observed at lower temperatures. These results indicate that electrochemical

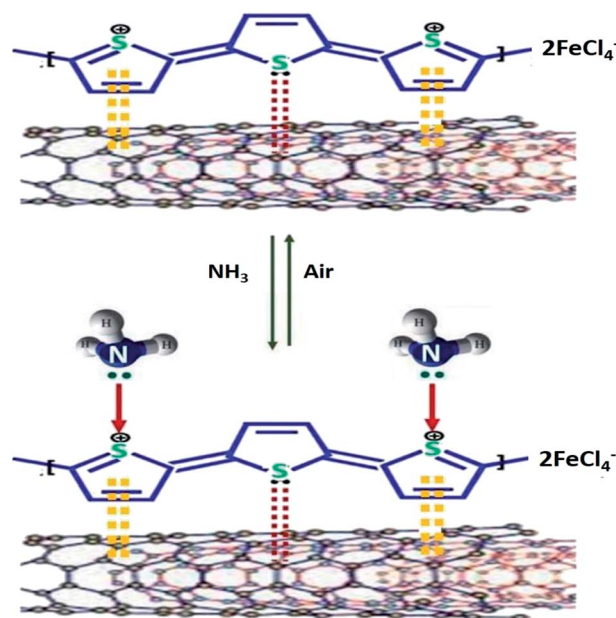


Fig. 22 Shows the proposed mechanism of the interaction of  $\text{NH}_3$  with PTh/MWCNTs nanocomposite. Reproduced from ref. 202, copyright 2020, Elsevier.





Table 4 Summary of sensing performance of certain conductive polymer/CNTs towards different analytes

Analyte	Conductive polymer	CNTs composition limit	Operating temperature	Detection range	Performance	Ref.
<b>Chemical warfare stimulant</b>						
DMMP	PANI (SWNT)	—	Room temperature	1 to 10 ppm	Response: 27.1%, response time: 5.5 s, gas concentration: 10 ppm	203
	PANI (MWCNT)	1 wt%	50 °C	332 to 800 ppm	Response: 1%, gas concentration: 332 ppm	204
	PPy (Co <sub>3</sub> O <sub>4</sub> @Au/MWCNT)	6.5 wt%	Room temperature	20 to 120 ppm	Response: 98%, response time: 60 s, recovery time: 439 s, gas concentration: 120 ppm	188
Malathion	PANI (SWNT)	—	Room temperature	2.0 × 10 <sup>-7</sup> M to 14.0 × 10 <sup>-7</sup> M	Recovery: 100.002%	205
<b>Toxic gases</b>						
NO <sub>2</sub>	PTh (SWCNT)	—	Room temperature	0.01 to 10 ppm	Response: 28%, response time: 330 s, gas concentration: 10 ppm	206
DCM	PANI (MWCNT)	1 wt%	50 °C	481 to 1442 ppm	Response time: 200 s, gas concentration: 1442 ppm	204
<b>Volatile organic compounds (VOC)</b>						
Ammonia	PANI	—	Room temperature	4 to 30 ppm	Response: 418%, gas concentration: 4 ppm, response time: 167 s, recovery time: 379 s	207
	PANI (MWCNT)	—	Room temperature	2 to 10 ppm	Response time: 6 s, recovery time: 6 s	173
	PANI (MWCNT)	5 mg	Room temperature	0.2 to 15 ppm	Response time: 67 s, gas concentration: 12 ppm	208
	PANI (SWCNT)	1 mg mL <sup>-1</sup> in 0.5 mL aqueous solution	Room temperature	0 to 500 ppm	Response: 2.44%	200
Nitrotoluene	Poly(TPP) (SWCNT)	0.2 µL drop – until desired resistance achieved	Room temperature	50 to 230 000 ppm	Response time: 8 min, gas concentration: 9 ppm	209
Acetone	Poly(TPP) (SWCNT)	0.2 µL drop – until desired resistance achieved	Room temperature	50 to 230 000 ppm	Response: 0.25%, gas concentration: 9 ppm	209
Formaldehyde	Polyethyleneimine (SWCNT)	—	Room temperature	0 to 0.80 ppm	Gas concentration: 20 ppb, response time: 18 s, response: 95%	210
H <sub>2</sub>	PANI (MWCNT)	4 wt%	Room temperature	—	Response > 20%	211



functionalisation of SWNTs provides a promising new method of creating highly advanced nano sensors with improved sensitivity, detection limit, and reproducibility. Fig. 19 shows the schematic diagram of PANI coated with SWCNT-COOH on interdigitated electrodes on the Si substrate. Fig. 20 shows SEM images of a bare SWCNT before and after electropolymerisation, and their NH<sub>3</sub> sensitivity (PANI was coated on SWCNT-COOH using a two-electrode configuration at 0.8 V for 5 minutes).

An interesting study of PTh-based/SWCNT on the detection of *n*-methylphenethylamine (NMPEA) vapour, one of the most widespread, harmful and addictive illegal drugs in the world, was conducted by Zhang *et al.* (2018).<sup>201</sup> The regioregular poly[3-(6-carboxyhexyl)thiophene-2,5-diyl] (P3CT) and regioregular poly(3-octylthiophene-2,5-diyl) (P3OT) (Fig. 21) was used in the study and was non-covalently functionalised with SWCNTs. NMPEA was detected at concentrations of as low as 4 ppb exposure. Results found that the acid-base interaction between the amine compounds and the carboxylic acid groups in the polymer contributed to extraordinary sensitivity of the P3CT/CNT sensor towards amine compounds, where the carboxylic acid group in the P3CT acted as a receptor of amine compounds and enhanced the interaction between the amine compounds and the sensor materials. The sensors were also able to distinguish NMPEA from two other amine compounds, various volatile chemical compounds (VOCs), and water vapour by observing the recoverability of the sensor's signal after exposure even when the vapour concentrations of amines were several orders of magnitude lower than those of the VOCs.

Another study was done by Hussain *et al.* (2020) on the electrical conductivity and NH<sub>3</sub> sensing for PTh/MWCNTs nanocomposites.<sup>202</sup> The performance of PTh/MWCNTs nanocomposites showed significantly enhanced electrical conductivity, where PTh/MWCNTs-3 (PTh/MWCNTs nanocomposite containing 15% MWCNTs to the weight of monomers) was found to be an ultra-sensitive (detection limit of 0.1 ppm), completely reversible, highly selective, and stable ammonia sensor at room temperature. The sensing response of PTh/MWCNTs-3 at 2000, 1500, 1000, 500, 400, 200, 100, 50, 1, and 0.1 ppm of NH<sub>3</sub> was found to be 88.70%, 73.27%, 62.04%, 51.65%, 46.96%, 42.97%, 38.86%, 35.18%, 32.93%, and 27.66%, respectively. The results showed that relative humidity only had a small effect on NH<sub>3</sub> sensing properties of PTh/MWCNTs-3. Fig. 22 shows the proposed mechanism of the interaction of NH<sub>3</sub> with PTh/MWCNTs nanocomposite. Table 4 shows the summary of sensing performance of certain conductive polymer/CNTs towards different analytes.

## 6. Conclusions and future outlook

CNT has prominent mechanical and electrical properties as well as good electron transport properties which prove that the development of CNT/polymer nanocomposites could contribute in expanding many areas of applications. The deficiencies from these nanocomposites need to be solved, such as lack of stability, solubility, selectivity, and poor interfacial adhesion between CNT and polymers. From recent studies and journals, a lot of

strategies and efforts have been discussed to functionalise the paramount discovery of interaction between CNT and polymers. Still, the application of CNT in real products are still in early stage of realisation but has a bright future for a new industrialisation era. It was introduced that either pristine or functionalised CNT may change the properties of conductive polymer matrices. Some factors, such as the shape, size, type, aspect ratio, dispersion, and alignment of CNT within the nanocomposite affect the properties of nanocomposites. Here, covalent functionalisation of CNTs modified the stacking and layering properties of CNT mostly by changing the hydrogen bonding by reduction of van der Waals interactions between the CNTs and led to debundling of the tubes which contribute to the well dispersion of CNTs and good sensitivity towards analytes. In general, the attachment of carboxylic, hydroxyl, polymer, and other hydrophilic groups help in improving the chemical structure of CNTs by filling in the defect sites, thus improving the conductivity and charge transfer of the nanocomposites. In addition, the main advantages of CNT functionalisation with polymer are to ensure uniform dispersion of the nanocomposites and prevent the accumulation and agglomeration of CNTs which happens through attraction-depletion of the CNT itself. The nanocomposites are synthesised through chemical oxidative polymerisation, electrochemical oxidative polymerisation, and direct solution-mixing methods. Therefore, *in situ* polymerisation is one of the efficient methods to obtain uniform dispersion of CNTs in a thermosetting polymer. The aforementioned method involves the addition or condensation reactions of the monomers with CNTs. Melt blending, latex technology, and simpler solution mixing are other ways to fabricate CNT/polymers. More facile and efficient methods need to be developed for a better future.

One of the nanocomposites applications highlighted is chemical sensor. The infamous one is the CNT-based chemiresistive gas sensor. In the light of this approach, CNT/conductive polymers nanocomposites synergise the construction of better transducer, acquired the simplicity, rapid response, and low-cost process. Generally, the sensor translates chemical interaction between the receptors and analytes into changing electrical resistance, a simple electric signal to be analysed. The detection performance is exploited by the chemical composition and structure, conductivity and charge transport, along with its adsorption ability. At this juncture, the parameters need to be considered for sensor performance are sensitivity, analyte concentration, operation temperature, limit of detection, recovery time, response time, response, and selectivity. Even if the behaviour and composition of CNTs and the properties of CNT/conductive polymer are well understood, still, there are many hitherto fundamental arguments about nanocomposites that need to be discovered, such as techniques in fabrication of gas sensor, modifications and functionalisation of CNTs, the charge transfer in nanocomposites, processing cost as well as introduction of graphene in gas sensing. Further studies are paramount to discover each property and interaction on CNT-based nanocomposites.

## Conflicts of interest

There are no conflicts to declare.



## Acknowledgements

Financial support from Newton fund's Program and Malaysia Partnership and Alliances in Research (MyPAiR) for ISIS-NEWTON/2019/SG/01 and Chemical Defence Research Centre (CHEMDEF) for a research grant (UPNM/2018/CHEMDEFF/ST/3) are gratefully acknowledged.

## References

- 1 S. Iijima, Helical microtubules of graphitic carbon, *Nature*, 1991, **354**, 56–58.
- 2 B. De, S. Banerjee, K. D. Verma, T. Pal, P. K. Manna and K. K. Kar, Carbon nanotube as electrode materials for supercapacitors, *Handbook of Nanocomposite Supercapacitor Materials II*, Springer, 2020, pp. 229–43.
- 3 M. Ahmadi, O. Zabihi, M. Masoomi and M. Naebe, Synergistic effect of MWCNTs functionalization on interfacial and mechanical properties of multi-scale UHMWPE fibre reinforced epoxy composites, *Compos. Sci. Technol.*, 2016, **134**, 1–11.
- 4 B. Maruyama and K. Alam, Carbon nanotubes and nanofibers in composite materials, *SAMPE J.*, 2002, **38**, 59–70.
- 5 P. G. Collins and P. Avouris, *Nanotubes for Electronics – Scientific American*, Nature Publishing Group, San Francisco, 2000, vol. 283, pp. 62–69.
- 6 Z. Wu, Z. Yang, K. Pei, X. Qian, C. Jin and R. Che, Dandelion-like carbon nanotube assembly embedded with closely separated Co nanoparticles for high-performance microwave absorption materials, *Nanoscale*, 2020, **12**, 10149–10157.
- 7 Z. Mo, R. Yang, D. Lu, L. Yang, Q. Hu, H. Li, *et al.*, Lightweight, three-dimensional carbon Nanotube@TiO<sub>2</sub> sponge with enhanced microwave absorption performance, *Carbon*, 2019, **144**, 433–439.
- 8 L. F. C. Souto and B. G. Soares, Polyaniline/carbon nanotube hybrids modified with ionic liquids as anticorrosive additive in epoxy coatings, *Prog. Org. Coat.*, 2020, **143**, 105598.
- 9 A. G. Hassan, M. A. M. Yajid, S. N. Saud, T. A. A. Bakar, A. Arshad and N. Mazlan, Effects of varying electrodeposition voltages on surface morphology and corrosion behavior of multi-walled carbon nanotube coated on porous Ti-30 at%-Ta shape memory alloys, *Surf. Coat. Technol.*, 2020, **401**, 126257.
- 10 R. O. Medupin, O. K. Abubakre, A. S. Abdulkareem, R. A. Muriana and A. S. Abdulrahman, Carbon Nanotube Reinforced Natural Rubber Nanocomposite for Anthropomorphic Prosthetic Foot Purpose, *Sci. Rep.*, 2019, **9**, 1–11.
- 11 M. S. Z. Abidin, T. Herceg, E. S. Greenhalgh, M. Shaffer and A. Bismarck, Enhanced fracture toughness of hierarchical carbon nanotube reinforced carbon fibre epoxy composites with engineered matrix microstructure, *Compos. Sci. Technol.*, 2019, **170**, 85–92.
- 12 D. Feng, D. Xu, Q. Wang and P. Liu, Highly stretchable electromagnetic interference (EMI) shielding segregated polyurethane/carbon nanotube composites fabricated by microwave selective sintering, *J. Mater. Chem. C*, 2019, **7**, 7938–7946.
- 13 E. Zhou, J. Xi, Y. Guo, Y. Liu, Z. Xu, L. Peng, *et al.*, Synergistic effect of graphene and carbon nanotube for high-performance electromagnetic interference shielding films, *Carbon*, 2018, **133**, 316–322.
- 14 M. Chen, Q. S. Jing, H. B. Sun, J. Q. Xu, Z. Y. Yuan, J. T. Ren, *et al.*, Engineering the Core-Shell-Structured NCNTs-Ni<sub>2</sub>Si@Porous Si Composite with Robust Ni-Si Interfacial Bonding for High-Performance Li-Ion Batteries, *Langmuir*, 2019, **35**, 6321–6332.
- 15 F. Guo, T. Kang, Z. Liu, B. Tong, L. Guo, Y. Wang, *et al.*, Advanced Lithium Metal-Carbon Nanotube Composite Anode for High-Performance Lithium-Oxygen Batteries, *Nano Lett.*, 2019, **19**, 6377–6384.
- 16 M. Chen, G. C. Wang, W. Q. Yang, Z. Y. Yuan, X. Qian, J. Q. Xu, *et al.*, Enhanced synergistic catalytic effect of Mo<sub>2</sub>C/NCNTs@Co heterostructures in dye-sensitized solar cells: fine-tuned energy level alignment and efficient charge transfer behavior, *ACS Appl. Mater. Interfaces*, 2019, **11**, 42156–42171.
- 17 M. Chen, G. C. Wang, L. L. Shao, Z. Y. Yuan, X. Qian, Q. S. Jing, *et al.*, Strategic Design of Vacancy-Enriched Fe<sub>1-x</sub>S Nanoparticles Anchored on Fe<sub>3</sub>C-Encapsulated and N-Doped Carbon Nanotube Hybrids for High-Efficiency Triiodide Reduction in Dye-Sensitized Solar Cells, *ACS Appl. Mater. Interfaces*, 2018, **10**, 31208–31224.
- 18 M. Chen, G. Zhao, L. L. Shao, Z. Y. Yuan, Q. S. Jing, K. J. Huang, *et al.*, Controlled synthesis of nickel encapsulated into nitrogen-doped carbon nanotubes with covalent bonded interfaces: the structural and electronic modulation strategy for an efficient electrocatalyst in dye-sensitized solar cells, *Chem. Mater.*, 2017, **29**, 9680–9694.
- 19 M. Chen, L. L. Shao, X. W. Lv, G. C. Wang, W. Q. Yang, Z. Y. Yuan, *et al.*, In situ growth of Ni-encapsulated and N-doped carbon nanotubes on N-doped ordered mesoporous carbon for high-efficiency triiodide reduction in dye-sensitized solar cells, *Chem. Eng. J.*, 2020, 124633.
- 20 N. Janudin, N. Abdullah, F. M. Yasin, M. H. Yaacob, M. Z. Ahmad, L. C. Abdullah, *et al.*, Low cost and room temperature methane detection using multi walled-carbon nanotubes functionalized with octadecanol, *ZULFAQAR Journal of Defence Science, Engineering & Technology*, 2018, **1**.
- 21 N. Janudin, N. Abdullah, W. M. Z. Wan Yunus, F. M. Yasin, M. H. Yaacob, N. Mohamad Saidi, *et al.*, Effect of functionalized carbon nanotubes in the detection of benzene at room temperature, *J. Nanotechnol.*, 2018, **2018**, 1–7.
- 22 D. Maity, K. Rajavel and R. T. R. Kumar, Polyvinyl alcohol wrapped multiwall carbon nanotube (MWCNTs) network on fabrics for wearable room temperature ethanol sensor, *Sens. Actuators, B*, 2018, **261**, 297–306.



- 23 V. Schroeder, S. Savagatrup, M. He, S. Lin and T. M. Swager, Carbon nanotube chemical sensors, *Chem. Rev.*, 2018, **119**, 599–663.
- 24 M. S. Yahya and M. Ismail, Improvement of hydrogen storage properties of MgH<sub>2</sub> catalyzed by K<sub>2</sub>NbF<sub>7</sub> and multiwall carbon nanotube, *J. Phys. Chem. C*, 2018, **122**, 11222–11233.
- 25 M. Mananghaya, D. Yu, G. N. Santos and E. Rodulfo, Scandium and titanium containing single-walled carbon nanotubes for hydrogen storage: a thermodynamic and first principle calculation, *Sci. Rep.*, 2016, **6**, 27370.
- 26 S. Park, A. P. Gupta, S. J. Yeo, J. Jung, S. H. Paik, M. Mativenga, *et al.*, Carbon nanotube field emitters synthesized on metal alloy substrate by PECVD for customized compact field emission devices to be used in X-ray source applications, *Nanomaterials*, 2018, **8**, 378.
- 27 Y. Song, J. Li, Q. Wu, C. Yi, H. Wu, Z. Chen, *et al.*, Study of film thickness effect on carbon nanotube based field emission devices, *J. Alloys Compd.*, 2020, **816**, 152648.
- 28 M. Chen and L. L. Shao, Review on the recent progress of carbon counter electrodes for dye-sensitized solar cells, *Chem. Eng. J.*, 2016, **304**, 629–645.
- 29 S. Z. N. Demon, A. I. Kamisan, N. Abdullah, S. A. M. Noor, O. K. Khim, N. A. M. Kasim, *et al.*, Graphene-based Materials in Gas Sensor Applications: A Review, *Sens. Mater.*, 2020, **32**, 759–777.
- 30 M. Chen, R. H. Zha, Z. Y. Yuan, Q. S. Jing, Z. Y. Huang, X. K. Yang, *et al.*, Boron and phosphorus co-doped carbon counter electrode for efficient hole-conductor-free perovskite solar cell, *Chem. Eng. J.*, 2017, **313**, 791–800.
- 31 M. Chen, L. L. Shao, Y. X. Guo and X. Q. Cao, Nitrogen and phosphorus co-doped carbon nanosheets as efficient counter electrodes of dye-sensitized solar cells, *Chem. Eng. J.*, 2016, **304**, 303–312.
- 32 M. Chen, L. L. Shao, Y. Xia, Z. Y. Huang, D. L. Xu, Z. W. Zhang, *et al.*, Construction of highly catalytic porous TiOPC nanocomposite counter electrodes for dye-sensitized solar cells, *ACS Appl. Mater. Interfaces*, 2016, **8**, 26030–26040.
- 33 M. Chen, L. L. Shao, Z. Y. Yuan, Q. S. Jing, K. J. Huang, Z. Y. Huang, *et al.*, General strategy for controlled synthesis of Ni<sub>x</sub>P<sub>y</sub>/carbon and its evaluation as a counter electrode material in dye-sensitized solar cells, *ACS Appl. Mater. Interfaces*, 2017, **9**, 17949–17960.
- 34 M. Chen, L. L. Shao, X. Qian, T. Z. Ren and Z. Y. Yuan, Direct synthesis of cobalt nanoparticle-embedded mesoporous carbons for high-performance dye-sensitized solar cell counter electrodes, *J. Mater. Chem. C*, 2014, **2**, 10312–10321.
- 35 W. Yang, S. Mao, J. Yang, T. Shang, H. Song, J. Mabon, *et al.*, Large-deformation and high-strength amorphous porous carbon nanospheres, *Sci. Rep.*, 2016, **6**, 24187.
- 36 B. Alemour, M. H. Yaacob, H. N. Lim and M. R. Hassan, Review of Electrical Properties of Graphene Conductive Composites, *Int. J. Nanoelectron. Mater.*, 2018, **11**, 371–398.
- 37 AZoM, *Graphite (C) - Classifications, Properties & Applications*, Azo Materials, 2002, available from: <https://www.azom.com>.
- 38 L. F. Castañeda, F. C. Walsh, J. L. Nava and C. P. de Leon, Graphite felt as a versatile electrode material: properties, reaction environment, performance and applications, *Electrochim. Acta*, 2017, **258**, 1115–1139.
- 39 M. E. Spahr, S. Zürcher, M. Rodlert-bacilieri, F. Mornaghini and T. M. Gruenberger, High-conductive carbon black with low viscosity, *US Pat.*, US2018015552A1, 2018.
- 40 W. Lu, T. He, B. Xu, X. He, H. Adidharma, M. Radosz, *et al.*, Progress in catalytic synthesis of advanced carbon nanofibers, *J. Mater. Chem. A*, 2017, **5**, 13863–13881.
- 41 D. Burton, P. Lake and A. Palmer, *AIP Conf. Proc.*, 2020, **2068**(1), 020061.
- 42 M. Kavitha and A. M. Kalpana, Carbon Nanotubes: Properties and Applications-A Brief Review, *i-manager's Journal on Electronics Engineering*, 2017, **7**, 1.
- 43 K. R. Reddy, B. C. Sin, C. H. Yoo, W. Park, K. S. Ryu, J. S. Lee, *et al.*, A new one-step synthesis method for coating multi-walled carbon nanotubes with cuprous oxide nanoparticles, *Scr. Mater.*, 2008, **58**, 1010–1013.
- 44 H. J. Choi, K. Zhang and J. Y. Lim, Multi-Walled Carbon Nanotube/Polystyrene Composites Prepared by in situ Bulk Sonochemical Polymerization, *J. Nanosci. Nanotechnol.*, 2007, **7**, 3400–3403.
- 45 A. Cwirzen, K. Habermehl-Cwirzen and V. Penttala, Surface decoration of carbon nanotubes and mechanical properties of cement/carbon nanotube composites, *Adv. Cem. Res.*, 2008, **20**, 65–73.
- 46 H. H. So, J. W. Cho and N. G. Sahoo, Effect of carbon nanotubes on mechanical and electrical properties of polyimide/carbon nanotubes nanocomposites, *Eur. Polym. J.*, 2007, **43**, 3750–3756.
- 47 I. A. Kinloch, J. Suhr, J. Lou, R. J. Young and P. M. Ajayan, Composites with carbon nanotubes and graphene: an outlook, *Science*, 2018, **362**, 547–553.
- 48 X. Zhang, W. Lu, G. Zhou and Q. Li, Understanding the mechanical and conductive properties of carbon nanotube fibers for smart electronics, *Adv. Mater.*, 2020, **32**, 1902028.
- 49 X. Yao, X. Gao, J. Jiang, C. Xu, C. Deng and J. Wang, Comparison of carbon nanotubes and graphene oxide coated carbon fiber for improving the interfacial properties of carbon fiber/epoxy composites, *Composites, Part B*, 2018, **132**, 170–177.
- 50 H. Wei, Y. Wang, J. Guo, B. Qiu, D. Ding, S. Wei, *et al.*, Synthesis of Multifunctional Carbon Nanostructures, *Handbook of Carbon Nano Materials (Volumes 7–8)*, 2015, vol. 7, p. 89.
- 51 M. A. Morsi, A. Rajeh and A. A. Al-Muntaser, Reinforcement of the optical, thermal and electrical properties of PEO based on MWCNTs/Au hybrid fillers: nanodielectric materials for organoelectronic devices, *Composites, Part B*, 2019, **173**, 106957.
- 52 N. S. N. Sa'aya, S. Z. N. Demon, N. Abdullah, V. F. K. E. Abd Shatar and N. A. Halim, Optical and Morphological Studies



- of Multiwalled Carbon Nanotube-incorporated Poly(3-hexylthiophene-2, 5-diyl) Nanocomposites, *Sens. Mater.*, 2019, **31**, 2997–3006.
- 53 S. Bose, R. A. Khare and P. Moldenaers, Assessing the strengths and weaknesses of various types of pre-treatments of carbon nanotubes on the properties of polymer/carbon nanotubes composites: a critical review, *Polymer*, 2010, **51**, 975–993.
- 54 H. Li, D. Yuan, P. Li and C. He, High conductive and mechanical robust carbon nanotubes/waterborne polyurethane composite films for efficient electromagnetic interference shielding, *Composites, Part A*, 2019, **121**, 411–417.
- 55 L. Chen, X. J. Pang, M. Z. Qu, Q. T. Zhang, B. Wang, B. L. Zhang, *et al.*, Fabrication and characterization of polycarbonate/carbon nanotubes composites, *Composites, Part A*, 2006, **37**, 1485–1489.
- 56 Y. Wang, X. Zhang, S. You and Y. Hu, One-step electrosynthesis of visible light responsive double-walled alloy titanium dioxide nanotube arrays for use in photocatalytic degradation of dibutyl phthalate, *RSC Adv.*, 2020, **10**, 21238–21247.
- 57 Y. Cheng, J. Cao, H. Lv, H. Zhao, Y. Zhao and G. Ji, In situ regulating aspect ratio of bamboo-like CNTs via  $\text{Co}_x\text{Ni}_{1-x}$ -catalyzed growth to pursue superior microwave attenuation in X-band, *Inorg. Chem. Front.*, 2019, **6**, 309–316.
- 58 X. Wei, X. Cao, Y. Wang, G. Zheng, K. Dai, C. Liu, *et al.*, Conductive herringbone structure carbon nanotube/thermoplastic polyurethane porous foam tuned by epoxy for high performance flexible piezoresistive sensor, *Compos. Sci. Technol.*, 2017, **149**, 166–177.
- 59 J. L. Delgado, M. Á. Herranz and N. Martin, The nano-forms of carbon, *J. Mater. Chem.*, 2008, **18**, 1417–1426.
- 60 J. L. Delgado, M. A. Herranz and N. Martin, The nano-forms of carbon, *J. Mater. Chem.*, 2008, **18**, 1417–1426.
- 61 Y. Zhang, L. Liu, B. Van der Bruggen and F. Yang, Nanocarbon based composite electrodes and their application in microbial fuel cells, *J. Mater. Chem. A*, 2017, **5**, 12673–12698.
- 62 Y. Liu, J. Zhang, Y. Cheng and S. P. Jiang, Effect of carbon nanotubes on direct electron transfer and electrocatalytic activity of immobilized glucose oxidase, *ACS Omega*, 2018, **3**, 667–676.
- 63 J. Wang, Carbon-nanotube based electrochemical biosensors: a review, *Electroanalysis*, 2005, **17**, 7–14.
- 64 C. B. Jacobs, M. J. Peairs and B. J. Venton, Carbon nanotube based electrochemical sensors for biomolecules, *Anal. Chim. Acta*, 2010, **662**, 105–127.
- 65 P. C. Ma, N. A. Siddiqui, G. Marom and J. K. Kim, Dispersion and functionalization of carbon nanotubes for polymer-based nanocomposites: a review, *Composites, Part A*, 2010, **41**, 1345–1367.
- 66 R. I. Rubel, M. H. Ali, M. A. Jafor and M. M. Alam, Carbon nanotubes agglomeration in reinforced composites: a review, *AIMS Mater. Sci.*, 2019, **6**, 756.
- 67 S. M. Sabet, H. Mahfuz, A. C. Terentis, M. Nezakat and J. Hashemi, Effects of POSS functionalization of carbon nanotubes on microstructure and thermomechanical behavior of carbon nanotube/polymer nanocomposites, *J. Mater. Sci.*, 2018, **53**, 8963–8977.
- 68 G. J. Bahun, C. Wang and A. Adronov, Solubilizing single-walled carbon nanotubes with pyrene-functionalized block copolymers, *J. Polym. Sci., Part A: Polym. Chem.*, 2006, **44**, 1941–1951.
- 69 Y. L. Zhao and J. F. Stoddart, Noncovalent functionalization of single-walled carbon nanotubes, *Acc. Chem. Res.*, 2009, **42**, 1161–1171.
- 70 R. Konnola and K. Joseph, Effect of side-wall functionalisation of multi-walled carbon nanotubes on the thermo-mechanical properties of epoxy composites, *RSC Adv.*, 2016, **6**, 23887–23899.
- 71 Y. Zhang and S. Huang, Significant improvements in the mechanical properties of chitosan functionalized carbon nanotubes/epoxy composites, *RSC Adv.*, 2016, **6**, 26210–26215.
- 72 J. Chen, L. Yan, W. Song and D. Xu, Interfacial characteristics of carbon nanotube-polymer composites: a review, *Composites, Part A*, 2018, **114**, 149–169.
- 73 K. P. Maity, A. Patra and V. Prasad, Influence of the chemical functionalization of carbon nanotubes on low temperature ac conductivity with polyaniline composites, *J. Phys. D: Appl. Phys.*, 2020, **53**, 125303.
- 74 A. F. Quintero-Jaime, D. Cazorla-Amorós and E. Morallón, Electrochemical functionalization of single wall carbon nanotubes with phosphorus and nitrogen species, *Electrochim. Acta*, 2020, **340**, 135935.
- 75 O. I. Nakonechna, N. N. Belyavina, M. M. Dashevskiy, K. O. Ivanenko and S. L. Revo, Novel  $\text{Ti}_2\text{CuC}_x$  and  $\text{Ti}_3\text{Cu}_2\text{C}_x$  Carbides Obtained by Sintering of Products of Mechanochemical Synthesis of Ti, Cu and Carbon Nanotubes, *Phys. Chem. Org. Solid State*, 2018, **19**, 179–185.
- 76 M. G. Trulli, E. Sardella, F. Palumbo, G. Palazzo, L. C. Giannossa, A. Mangone, *et al.*, Towards highly stable aqueous dispersions of multi-walled carbon nanotubes: the effect of oxygen plasma functionalization, *J. Colloid Interface Sci.*, 2017, **491**, 255–264.
- 77 B. Singh, S. Lohan, P. S. Sandhu, A. Jain and S. K. Mehta, Functionalized carbon nanotubes and their promising applications in therapeutics and diagnostics, *Nanobiomater. Med. Imaging*, 2016, 455–478.
- 78 S. Ajori, R. Ansari and M. Darvizeh, Vibration characteristics of single-and double-walled carbon nanotubes functionalized with amide and amine groups, *Phys. B*, 2015, **462**, 8–14.
- 79 R. Afrin and N. A. Shah, Room temperature gas sensors based on carboxyl and thiol functionalized carbon nanotubes buckypapers, *Diamond Relat. Mater.*, 2015, **60**, 42–49.
- 80 N. Janudin, L. C. Abdullah, N. Abdullah, F. M. Yasin, N. M. Saidi and N. A. M. Kasim, Characterization of Amide and Ester Functionalized Multiwalled Carbon Nanotubes, *Asian J. Chem.*, 2018, **30**, 1613–1616.





- 81 K. Balasubramanian and M. Burghard, Chemically functionalized carbon nanotubes, *Small*, 2005, **1**, 180–192.
- 82 S. Kumar, R. Rani, N. Dilbaghi, K. Tankeshwar and K. H. Kim, Carbon nanotubes: a novel material for multifaceted applications in human healthcare, *Chem. Soc. Rev.*, 2017, **46**, 158–196.
- 83 J. Azadmanjiri, V. K. Srivastava, P. Kumar, M. Nikzad, J. Wang and A. Yu, Two- and three-dimensional graphene-based hybrid composites for advanced energy storage and conversion devices, *J. Mater. Chem. A*, 2018, **6**, 702–734.
- 84 B. Ribeiro, E. C. Botelho, M. L. Costa and C. F. Bandeira, Carbon nanotube buckypaper reinforced polymer composites: a review, *Polímeros*, 2017, **27**, 247–255.
- 85 S. Mallakpour and S. Soltanian, Surface functionalization of carbon nanotubes: fabrication and applications, *RSC Adv.*, 2016, **6**, 109916–109935.
- 86 N. Janudin, N. Abdullah, W. M. Z. W. Yunus, F. M. Yasin, M. H. Yaacob, N. Kasim, *et al.*, Carbon nanofibers functionalized with amide group for ammonia gas detection, *AIP Conf. Proc.*, 2019, **2068**, 020061.
- 87 S. A. Shamsuddin, M. N. Derman, U. Hashim, M. Kashif, T. Adam, N. H. A. Halim, *et al.*, Nitric acid treated multi-walled carbon nanotubes optimized by Taguchi method, *AIP Conf. Proc.*, 2016, **1756**, 090002.
- 88 P. I. Gonzalez-Chi, O. Rodríguez-Uicab, C. Martin-Barrera, J. Uribe-Calderon, G. Canché-Escamilla, M. Yazdani-Pedram, *et al.*, Influence of aramid fiber treatment and carbon nanotubes on the interfacial strength of polypropylene hierarchical composites, *Composites, Part B*, 2017, **122**, 16–22.
- 89 A. Zeino, A. Abulkibash, M. Khaled and M. Atieh, Bromate removal from water using doped iron nanoparticles on multiwalled carbon nanotubes (CNTs), *J. Nanomater.*, 2014, **2014**, 1–9.
- 90 T. Zhang, K. Xi, M. Gu and Z. S. Jiang, Phosphoryl choline-grafted water-soluble carbon nanotube, *Chin. Chem. Lett.*, 2008, **19**, 105–109.
- 91 C. A. Dyke and J. M. Tour, Covalent Functionalization of Single-Walled Carbon Nanotubes for Materials Applications, *J. Phys. Chem. A*, 2004, **108**, 11151–11159.
- 92 S. Goyanes, G. R. Rubiolo, A. Salazar, A. Jimeno, M. A. Corcuera and I. Mondragon, Carboxylation treatment of multiwalled carbon nanotubes monitored by infrared and ultraviolet spectroscopies and scanning probe microscopy, *Diamond Relat. Mater.*, 2007, **16**, 412–417.
- 93 J. Chen, M. A. Hamon, H. Hu, Y. Chen, A. M. Rao, P. C. Eklund, *et al.*, Solution properties of single-walled carbon nanotubes, *Science*, 1998, **282**, 95–98.
- 94 J. Zhang, H. Zou, Q. Qing, Y. Yang, Q. Li, Z. Liu, *et al.*, Effect of chemical oxidation on the structure of single-walled carbon nanotubes, *J. Phys. Chem. B*, 2003, **107**, 3712–3718.
- 95 E. Malikov, O. H. Akperov, M. B. Muradov, G. Eyvazova, A. M. Maharramov, A. Kukovec, *et al.*, Oxidation of multiwalled carbon nanotubes using different oxidation agents like nitric acid and potassium permanganate, *News Baku Univ.*, 2014, **4**, 49–59.
- 96 H. Korri-Youssoufi, B. Zribi, A. Miodek and A. M. Haghiri-Gosnet, Carbon-Based Nanomaterials for Electrochemical DNA Sensing, *Nanotechnology and Biosensors*, Elsevier, 2018, pp. 113–50.
- 97 M. Adamska and U. Narkiewicz, Fluorination of carbon nanotubes – a review, *J. Fluorine Chem.*, 2017, **200**, 179–189.
- 98 J. H. Kim, E. Jeong and Y. S. Lee, Characteristics of fluorinated CNTs added carbon foams, *Appl. Surf. Sci.*, 2016, **360**, 1009–1015.
- 99 H. F. Bettinger, Experimental and Computational Investigations of the Properties of Fluorinated Single-Walled Carbon Nanotubes, *ChemPhysChem*, 2003, **4**, 1283–1289.
- 100 H. Touhara, A. Yonemoto, K. Yamamoto, S. Komiyama, S. Kawasaki, F. Okino, *et al.*, Fluorination of cup-stacked carbon nanotubes, structures and properties, *MRS Online Proc. Libr.*, 2004, **858**, HH12.3.
- 101 A. Setaro, M. Adeli, M. Glaeske, D. Przyrembel, T. Bisswanger, G. Gordeev, *et al.*, Preserving  $\pi$ -conjugation in covalently functionalized carbon nanotubes for optoelectronic applications, *Nat. Commun.*, 2017, **8**, 1–7.
- 102 Z. Hu, Q. Shao, X. Xu, D. Zhang and Y. Huang, Surface initiated grafting of polymer chains on carbon nanotubes via one-step cycloaddition of diarylcarbene, *Compos. Sci. Technol.*, 2017, **142**, 294–301.
- 103 V. K. Abdelkader, S. Scelfo, C. García-Gallarín, M. L. Godino-Salido, M. Domingo-García, F. J. López-Garzón, *et al.*, Carbon tetrachloride cold plasma for extensive chlorination of carbon nanotubes, *J. Phys. Chem. C*, 2013, **117**, 16677–16685.
- 104 S. Zdanowska, M. Pyzalska, J. Drabowicz, D. Kulawik, V. Pavlyuk, T. Girek, *et al.*, Carbon nanotubes functionalized by salts containing stereogenic heteroatoms as electrodes in their battery cells, *Pol. J. Chem. Technol.*, 2016, **18**, 22–26.
- 105 Z. Zhou, E. K. Orcutt, H. C. Anderson and K. J. Stowers, Hydrogen surface modification of a carbon nanotube catalyst for the improvement of ethane oxidative dehydrogenation, *Carbon*, 2019, **152**, 924–931.
- 106 C. Ménard-Moyon, N. Izard, E. Doris and C. Mioskowski, Separation of semiconducting from metallic carbon nanotubes by selective functionalization with azomethine ylides, *J. Am. Chem. Soc.*, 2006, **128**, 6552–6553.
- 107 O. Olugbenga, D. Michael and I. Suny, Investigation on purification potential of multiwalled carbon nanotubes using organic-mineral acid mixture, *Nanosci. Nanoeng.*, 2018, **4**, 1–8.
- 108 T. J. Aitchison, M. Ginic-Markovic, J. G. Matison, G. P. Simon and P. M. Fredericks, Purification, cutting, and sidewall functionalization of multiwalled carbon nanotubes using potassium permanganate solutions, *J. Phys. Chem. C*, 2007, **111**, 2440–2446.
- 109 M. L. Sham and J. K. Kim, Surface functionalities of multi-wall carbon nanotubes after UV/ozone and TETA treatments, *Carbon*, 2006, **44**, 768–777.



- 110 R. Malik, C. McConnell, N. T. Alvarez, M. Haase, S. Gbordzoe and V. Shanov, Rapid, in situ plasma functionalization of carbon nanotubes for improved CNT/epoxy composites, *RSC Adv.*, 2016, **6**, 108840–108850.
- 111 P. C. Ma, J. K. Kim and B. Z. Tang, Functionalization of carbon nanotubes using a silane coupling agent, *Carbon*, 2006, **44**, 3232–3238.
- 112 J. Wang, H. Jia, L. Ding, L. Zhu, X. Dai, X. Fei, *et al.*, Utilization of silane functionalized carbon nanotubes-silica hybrids as novel reinforcing fillers for solution styrene butadiene rubber, *Polym. Compos.*, 2013, **34**, 690–696.
- 113 Z. Abousalman-Rezvani, P. Eskandari, H. Roghani-Mamaqani and M. Salami-Kalajahi, Functionalization of carbon nanotubes by combination of controlled radical polymerization and “grafting to” method, *Adv. Colloid Interface Sci.*, 2020, 102126.
- 114 F. A. Abuilawi, T. Laoui, M. Al-Harhi and M. A. Atieh, Modification and functionalization of multiwalled carbon nanotube (MWCNT) via Fischer esterification, *Arabian J. Sci. Eng.*, 2010, **35**, 37–48.
- 115 Z. Su, Y. Cheng, C. Li, Y. Xiong, L. Xiao, S. Chen, *et al.*, Dispersing gold nanoparticles on thiolated polyaniline-multiwalled carbon nanotubes for development of an indole-3-acetic acid amperometric immunosensor, *Nanoscale Adv.*, 2019, **1**, 3607–3613.
- 116 Y. Maeda, S. Minami, Y. Takehana, J. S. Dang, S. Aota, K. Matsuda, *et al.*, Tuning of the photoluminescence and up-conversion photoluminescence properties of single-walled carbon nanotubes by chemical functionalization, *Nanoscale*, 2016, **8**, 16916–16921.
- 117 K. Adachi and Y. Tsukahara, Surface modification of carbon nanotubes by anionic approach, *Curr. Opin. Chem. Eng.*, 2016, **11**, 106–113.
- 118 G. Ostojic and M. C. Hersam, Functionalization of carbon nanotubes with metallic moieties, *US Pat.*, US8562905B2, 2019.
- 119 W. F. Chan, E. Marand and S. M. Martin, Novel zwitterion functionalized carbon nanotube nanocomposite membranes for improved RO performance and surface anti-biofouling resistance, *J. Membr. Sci.*, 2016, **509**, 125–137.
- 120 J. Liu, R. Che, H. Chen, F. Zhang, F. Xia, Q. Wu, *et al.*, Microwave absorption enhancement of multifunctional composite microspheres with spinel Fe<sub>3</sub>O<sub>4</sub> cores and anatase TiO<sub>2</sub> shells, *Small*, 2012, **8**, 1214–1221.
- 121 C. L. Zhu, M. L. Zhang, Y. J. Qiao, G. Xiao, F. Zhang and Y. J. Chen, Fe<sub>3</sub>O<sub>4</sub>/TiO<sub>2</sub> core/shell nanotubes: synthesis and magnetic and electromagnetic wave absorption characteristics, *J. Phys. Chem. C*, 2010, **114**, 16229–16235.
- 122 V. Vatanpour, S. S. Madaeni, R. Moradian, S. Zinadini and B. Astinchap, Novel antibiofouling nanofiltration polyethersulfone membrane fabricated from embedding TiO<sub>2</sub> coated multiwalled carbon nanotubes, *Sep. Purif. Technol.*, 2012, **90**, 69–82.
- 123 C. Wang, H. Wu, F. Qu, H. Liang, X. Niu and G. Li, Preparation and properties of polyvinyl chloride ultrafiltration membranes blended with functionalized multi-walled carbon nanotubes and MWCNTs/Fe<sub>3</sub>O<sub>4</sub> hybrids, *J. Appl. Polym. Sci.*, 2016, **133**, 1–8.
- 124 T. Hertel, A. Hagen, V. Talalaev, K. Arnold, F. Hennrich, M. Kappes, *et al.*, Spectroscopy of single- and double-wall carbon nanotubes in different environments, *Nano Lett.*, 2005, **5**, 511–514.
- 125 L. Vaisman, H. D. Wagner and G. Marom, The role of surfactants in dispersion of carbon nanotubes, *Adv. Colloid Interface Sci.*, 2006, **128**, 37–46.
- 126 P. Bilalis, D. Katsigiannopoulos, A. Avgeropoulos and G. Sakellariou, Non-covalent functionalization of carbon nanotubes with polymers, *RSC Adv.*, 2014, **4**, 2911–2934.
- 127 X. Wang, L. Bai, S. Kong, Y. Song and F. Meng, Star-shaped supramolecular ionic liquid crystals based on pyridinium salts, *Liq. Cryst.*, 2019, **46**, 512–522.
- 128 J. Dai, R. M. F. Fernandes, O. Regev, E. F. Marques and I. Furó, Dispersing carbon nanotubes in water with amphiphiles: dispersant adsorption, kinetics, and bundle size distribution as defining factors, *J. Phys. Chem. C*, 2018, **122**, 24386–24393.
- 129 T. Fujigaya and N. Nakashima, Non-covalent polymer wrapping of carbon nanotubes and the role of wrapped polymers as functional dispersants, *Sci. Technol. Adv. Mater.*, 2015, **16**, 024802.
- 130 S. M. Ghoreishi, M. Behpour, S. Mousavi, A. Khoobi and F. S. Ghoreishi, Simultaneous electrochemical determination of dopamine, ascorbic acid and uric acid in the presence of sodium dodecyl sulphate using a multi-walled carbon nanotube modified carbon paste electrode, *RSC Adv.*, 2014, **4**, 37979–37984.
- 131 B. I. Kharisov, O. V. Kharissova and A. V. Dimas, The dispersion, solubilization and stabilization in “solution” of single-walled carbon nanotubes, *RSC Adv.*, 2016, **6**, 68760–68787.
- 132 X. Zeng, D. Yang, H. Liu, N. Zhou, Y. Wang, W. Zhou, *et al.*, Detecting and Tuning the Interactions between Surfactants and Carbon Nanotubes for Their High-Efficiency Structure Separation, *Adv. Mater. Interfaces*, 2018, **5**, 1700727.
- 133 M. V. Manilo, N. Lebovka and S. Barany, Combined effect of cetyltrimethylammonium bromide and laponite platelets on colloidal stability of carbon nanotubes in aqueous suspensions, *J. Mol. Liq.*, 2017, **235**, 104–110.
- 134 M. Park, J. Park, J. Lee and S. Y. Ju, Scaling of binding affinities and cooperativities of surfactants on carbon nanotubes, *Carbon*, 2018, **139**, 427–436.
- 135 A. Ishibashi and N. Nakashima, Strong chemical structure dependence for individual dissolution of single-walled carbon nanotubes in aqueous micelles of biosurfactants, *Bull. Chem. Soc. Jpn.*, 2006, **79**, 357–359.
- 136 T. Fujigaya, M. Okamoto and N. Nakashima, Design of an assembly of pyridine-containing polybenzimidazole, carbon nanotubes and Pt nanoparticles for a fuel cell electrocatalyst with a high electrochemically active surface area, *Carbon*, 2009, **47**, 3227–3232.
- 137 Y. C. Jung, H. H. Kim, Y. A. Kim, J. H. Kim, J. W. Cho, M. Endo, *et al.*, Optically active multi-walled carbon



- nanotubes for transparent, conductive memory-shape polyurethane film, *Macromolecules*, 2010, **43**, 6106–6112.
- 138 W. Khan, R. Sharma and P. Saini, Carbon nanotube-based polymer composites: synthesis, properties and applications, *Carbon Nanotubes: Curr. Prog. Their Polym. Compos.*, 2016, 1–46.
- 139 C. Backes, A. M. Abdelkader, C. Alonso, A. Andrieux-Ledier, R. Arenal, J. Azpeitia, *et al.*, Production and processing of graphene and related materials, *2D Materials*, 2020, **7**, 022001.
- 140 J. M. Benoit, B. Corraze, S. Lefrant, W. J. Blau and P. Bemier, Transport properties of PMMA-carbon nanotubes composites, *Synth. Met.*, 2001, **121**, 1215–1216.
- 141 Z. Spitalsky, D. Tasis, K. Papagelis and C. Galiotis, Carbon nanotube–polymer composites: chemistry, processing, mechanical and electrical properties, *Prog. Polym. Sci.*, 2010, **35**, 357–401.
- 142 Q. Wang, T. Wang, J. Wang, W. Guo, Z. Qian and T. Wei, Preparation of antistatic high-density polyethylene composites based on synergistic effect of graphene nanoplatelets and multi-walled carbon nanotubes, *Polym. Adv. Technol.*, 2018, **29**, 407–416.
- 143 A. Chafidz, F. H. Latief, U. A. Samad, A. Ajbar and W. Al-Masry, Nanoindentation creep, nano-impact, and thermal properties of multiwall carbon nanotubes–polypropylene nanocomposites prepared via melt blending, *Polym.-Plast. Technol. Eng.*, 2016, **55**, 1373–1385.
- 144 J. P. S. da Silva, B. G. Soares, S. Livi and G. M. O. Barra, Phosphonium-based ionic liquid as dispersing agent for MWCNT in melt-mixing polystyrene blends: rheology, electrical properties and EMI shielding effectiveness, *Mater. Chem. Phys.*, 2017, **189**, 162–168.
- 145 P. Sen, K. Suresh, R. V. Kumar, M. Kumar and G. Pugazhenthii, A simple solvent blending coupled sonication technique for synthesis of polystyrene (PS)/multi-walled carbon nanotube (MWCNT) nanocomposites: effect of modified MWCNT content, *J. Sci.*, 2016, **1**, 311–323.
- 146 A. Funck and W. Kaminsky, Polypropylene carbon nanotube composites by in situ polymerization, *Compos. Sci. Technol.*, 2007, **67**, 906–915.
- 147 Y. Xie, J. Zhao, Z. Le, M. Li, J. Chen, Y. Gao, *et al.*, Preparation and electromagnetic properties of chitosan-decorated ferrite-filled multi-walled carbon nanotubes/polythiophene composites, *Compos. Sci. Technol.*, 2014, **99**, 141–146.
- 148 M. Feng, R. Sun, H. Zhan and Y. Chen, Decoration of carbon nanotubes with CdS nanoparticles by polythiophene interlinking for optical limiting enhancement, *Carbon*, 2010, **48**, 1177–1185.
- 149 A. Mohamed, K. Trickett, S. Y. Chin, S. Cummings, M. Sagisaka, L. Hudson, *et al.*, Universal surfactant for water, oils, and CO<sub>2</sub>, *Langmuir*, 2010, **26**, 13861–13866.
- 150 A. Mohamed, A. K. Anas, S. A. Bakar, A. A. Aziz, M. Sagisaka, P. Brown, *et al.*, Preparation of multiwall carbon nanotubes (MWCNTs) stabilised by highly branched hydrocarbon surfactants and dispersed in natural rubber latex nanocomposites, *Colloid Polym. Sci.*, 2014, **292**, 3013–3023.
- 151 N. H. K. Azman, M. M. Ramli and S. S. M. Isa, A Review of hybridization of carbon nanotube into graphene for gas sensor application, *IOP Conf. Ser.: Mater. Sci. Eng.*, 2019, 1–8.
- 152 S. T. Navale, D. K. Bandgar, M. A. Chougule and V. B. Patil, Facile method of preparation of PbS films for NO<sub>2</sub> detection, *RSC Adv.*, 2015, **5**, 6518–6527.
- 153 S. J. Choi, D. M. Lee, H. Yu, J. S. Jang, M. H. Kim, J. Y. Kang, *et al.*, All-carbon fiber-based chemical sensor: improved reversible NO<sub>2</sub> reaction kinetics, *Sens. Actuators, B*, 2019, **290**, 293–301.
- 154 R. Tang, Y. Shi, Z. Hou and L. Wei, Carbon nanotube-based chemiresistive sensors, *Sensors*, 2017, **17**, 882.
- 155 A. A. Baharuddin, B. C. Ang, A. S. M. A. Haseeb, Y. C. Wong and Y. H. Wong, Advances in chemiresistive sensors for acetone gas detection, *Mater. Sci. Semicond. Process.*, 2019, **103**, 104616.
- 156 O. Lupan, V. Cretu, V. Postica, N. Ababii, O. Polonskyi, V. Kaidas, *et al.*, Enhanced ethanol vapour sensing performances of copper oxide nanocrystals with mixed phases, *Sens. Actuators, B*, 2016, **224**, 434–448.
- 157 Y. C. Wong, B. C. Ang, A. S. M. A. Haseeb, A. A. Baharuddin and Y. H. Wong, Conducting Polymers as Chemiresistive Gas Sensing Materials: A Review, *J. Electrochem. Soc.*, 2019, **167**, 037503.
- 158 D. R. Miller, S. A. Akbar and P. A. Morris, Nanoscale metal oxide-based heterojunctions for gas sensing: a review, *Sens. Actuators, B*, 2014, **204**, 250–272.
- 159 I. V. Zaporotskova, N. P. Boroznina, Y. N. Parkhomenko and L. V. Kozhitov, Carbon nanotubes: Sensor properties. A review, *Mod. Electron. Mater.*, 2016, **2**, 95–105.
- 160 L. Camilli and M. Passacantando, Advances on sensors based on carbon nanotubes, *Chemosensors*, 2018, **6**, 62.
- 161 J. W. Yoon and J. H. Lee, Toward breath analysis on a chip for disease diagnosis using semiconductor-based chemiresistors: recent progress and future perspectives, *Lab Chip*, 2017, **17**, 3537–3557.
- 162 J. V. Yakhmi, V. Saxena and D. K. Aswal, Conducting polymer sensors, actuators and field-effect transistors, *Funct. Mater.*, 2012, 61–110.
- 163 M. Ghodrati, A. Mir and A. Farmani, Carbon nanotube field effect transistors-based gas sensors, *Nanosensors for Smart Cities*, Elsevier, 2020, pp. 171–83.
- 164 M. Ghodrati, A. Farmani and A. Mir, Nanoscale sensor-based tunneling carbon nanotube transistor for toxic gases detection: a first-principle study, *IEEE Sens. J.*, 2019, **19**, 7373–7377.
- 165 N. Janudin, F. M. Yasin, N. Abdullah, M. H. Yaacob, M. Z. Ahmad, R. N. I. R. Othman, *et al.*, Carbon nanotubes-based gas sensor in detection of methane gas at room temperature, *ZULFAQAR Journal of Defence Science, Engineering & Technology*, 2018, 1.
- 166 G. Neri, First fifty years of chemoresistive gas sensors, *Chemosensors*, 2015, **3**, 1–20.



- 167 R. Abdel-Karim, Y. Reda and A. Abdel-Fattah, Nanostructured Materials-Based Nanosensors, *J. Electrochem. Soc.*, 2020, **167**, 037554.
- 168 L. A. Panes-Ruiz, M. Shaygan, Y. Fu, Y. Liu, V. Khavrus, S. Oswald, *et al.*, Toward highly sensitive and energy efficient ammonia gas detection with modified single-walled carbon nanotubes at room temperature, *ACS Sens.*, 2018, **3**, 79–86.
- 169 C. Piloto, *Carbon nanomaterials for room temperature gas sensing*, Queensland University of Technology, 2016.
- 170 C. Paoletti, M. He, P. Salvo, B. Melai, N. Calisi, M. Mannini, *et al.*, Room temperature amine sensors enabled by sidewall functionalization of single-walled carbon nanotubes, *RSC Adv.*, 2018, **8**, 5578–5585.
- 171 A. H. Al-Husseini, W. R. Saleh and A. Al-Sammarraie, A Specific NH<sub>3</sub> Gas Sensor of a Thick MWCNTs-OH Network for Detection at Room Temperature, *J. Nano Res.*, 2019, 98–108.
- 172 Y. Li, M. Hodak, W. Lu and J. Bernholc, Mechanisms of NH<sub>3</sub> and NO<sub>2</sub> detection in carbon-nanotube-based sensors: an ab initio investigation, *Carbon*, 2016, **101**, 177–183.
- 173 S. Abdulla, T. L. Mathew and B. Pullithadathil, Highly sensitive, room temperature gas sensor based on polyaniline-multiwalled carbon nanotubes (PANI/MWCNTs) nanocomposite for trace-level ammonia detection, *Sens. Actuators, B*, 2015, **221**, 1523–1534.
- 174 A. Husain, S. Ahmad, M. U. Shariq and M. M. A. Khan, Ultra-Sensitive, Highly Selective and Completely Reversible Ammonia Sensor Based on Polythiophene/SWCNT Nanocomposite, *Materialia*, 2020, 100704.
- 175 O. Hamouma, N. Kaur, D. Oukil, A. Mahajan and M. M. Chehimi, Paper strips coated with polypyrrole-wrapped carbon nanotube composites for chemi-resistive gas sensing, *Synth. Met.*, 2019, **258**, 116223.
- 176 M. L. Y. Sin, G. C. T. Chow, G. M. K. Wong, W. J. Li, P. H. W. Leong and K. W. Wong, Ultralow-power alcohol vapor sensors using chemically functionalized multiwalled carbon nanotubes, *IEEE Trans. Nanotechnol.*, 2007, **6**, 571–577.
- 177 Y. Wang and J. T. W. Yeow, A review of carbon nanotubes-based gas sensors, *J. Sens.*, 2009, **2009**, 1–24.
- 178 M. C. Petty, T. Nagase, H. Suzuki and H. Naito, Molecular Electronics, *Springer Handbook of Electronic and Photonic Materials*, Springer, 2017, p. 1.
- 179 B. Liu, X. Liu, Z. Yuan, Y. Jiang, Y. Su, J. Ma, *et al.*, A flexible NO<sub>2</sub> gas sensor based on polypyrrole/nitrogen-doped multiwall carbon nanotube operating at room temperature, *Sens. Actuators, B*, 2019, **295**, 86–92.
- 180 D. Zhang, X. Fan, X. Hao and G. Dong, Facile fabrication of polyaniline nanocapsule modified zinc oxide hexagonal microdiscs for H<sub>2</sub>S gas sensing applications, *Ind. Eng. Chem. Res.*, 2019, **58**, 1906–1913.
- 181 A. Husain, S. Ahmad and F. Mohammad, Synthesis, characterisation and ethanol sensing application of polythiophene/graphene nanocomposite, *Mater. Chem. Phys.*, 2020, **239**, 122324.
- 182 J. Ram, R. G. Singh, F. Singh, V. Kumar, V. Chauhan, R. Gupta, *et al.*, Development of WO<sub>3</sub>-PEDOT:PSS hybrid nanocomposites based devices for liquefied petroleum gas (LPG) sensor, *J. Mater. Sci.: Mater. Electron.*, 2019, **30**, 13593–13603.
- 183 A. Saaedi, P. Shabani and R. Yousefi, High performance of methanol gas sensing of ZnO/PANI nanocomposites synthesized under different magnetic field, *J. Alloys Compd.*, 2019, **802**, 335–344.
- 184 A. H. Shah, Applications of carbon nanotubes and their polymer nanocomposites for gas sensors, *Carbon Nanotubes: Curr. Prog. Their Polym. Compos.*, 2016, 459–494.
- 185 G. W. Hunter, S. Akbar, S. Bhansali, M. Daniele, P. D. Erb, K. Johnson, *et al.*, Editors' choice—critical review—a critical review of solid state gas sensors, *J. Electrochem. Soc.*, 2020, **167**, 037570.
- 186 A. Mora, F. Han and G. Lubineau, Estimating and understanding the efficiency of nanoparticles in enhancing the conductivity of carbon nanotube/polymer composites, *Results Phys.*, 2018, **10**, 81–90.
- 187 C. Liu, H. Tai, P. Zhang, Z. Yuan, X. Du, G. Xie, *et al.*, A high-performance flexible gas sensor based on self-assembled PANI-CeO<sub>2</sub> nanocomposite thin film for trace-level NH<sub>3</sub> detection at room temperature, *Sens. Actuators, B*, 2018, **261**, 587–597.
- 188 S. Ramesh, Y. J. Lee, S. Msolli, J. G. Kim, H. S. Kim and J. H. Kim, Synthesis of a Co<sub>3</sub>O<sub>4</sub>@gold/MWCNT/polypyrrole hybrid composite for DMMP detection in chemical sensors, *RSC Adv.*, 2017, **7**, 50912–50919.
- 189 J. Wan, Y. Si, C. Li and K. Zhang, Bisphenol a electrochemical sensor based on multi-walled carbon nanotubes/polythiophene/Pt nanocomposites modified electrode, *Anal. Methods*, 2016, **8**, 3333–3338.
- 190 J. N. Gavgani, H. S. Dehsari, A. Hasani, M. Mahyari, E. K. Shalamzari, A. Salehi, *et al.*, A room temperature volatile organic compound sensor with enhanced performance, fast response and recovery based on N-doped graphene quantum dots and poly(3,4-ethylenedioxythiophene)-poly(styrenesulfonate) nanocomposite, *RSC Adv.*, 2015, **5**, 57559–57567.
- 191 S. G. Bachhav and D. R. Patil, Study of polypyrrole-coated MWCNT nanocomposites for ammonia sensing at room temperature, *J. Mater. Sci. Chem. Eng.*, 2015, **3**, 30.
- 192 B. Philip, J. K. Abraham, A. Chandrasekhar and V. K. Varadan, Carbon nanotube/PMMA composite thin films for gas-sensing applications, *Smart Mater. Struct.*, 2003, **12**, 935.
- 193 Y. Fan, M. Burghard and K. Kern, Chemical defect decoration of carbon nanotubes, *Adv. Mater.*, 2002, **14**, 130–133.
- 194 K. H. An, S. Y. Jeong, H. R. Hwang and Y. H. Lee, Enhanced sensitivity of a gas sensor incorporating single-walled carbon nanotube–polypyrrole nanocomposites, *Adv. Mater.*, 2004, **16**, 1005–1009.
- 195 W. Zhang, S. Cao, Z. Wu, M. Zhang, Y. Cao, J. Guo, *et al.*, High-Performance Gas Sensor of Polyaniline/Carbon





- Nanotube Composites Promoted by Interface Engineering, *Sensors*, 2020, **20**, 149.
- 196 N. R. Tanguy, M. Thompson and N. Yan, A review on advances in application of polyaniline for ammonia detection, *Sens. Actuators, B*, 2018, **257**, 1044–1064.
- 197 S. Bai, Y. Tian, M. Cui, J. Sun, Y. Tian, R. Luo, *et al.*, Polyaniline@SnO<sub>2</sub> heterojunction loading on flexible PET thin film for detection of NH<sub>3</sub> at room temperature, *Sens. Actuators, B*, 2016, **226**, 540–547.
- 198 L. Xue, W. Wang, Y. Guo, G. Liu and P. Wan, Flexible polyaniline/carbon nanotube nanocomposite film-based electronic gas sensors, *Sens. Actuators, B*, 2017, **244**, 47–53.
- 199 P. Kar and A. Choudhury, Carboxylic acid functionalized multi-walled carbon nanotube doped polyaniline for chloroform sensors, *Sens. Actuators, B*, 2013, **183**, 25–33.
- 200 T. Zhang, M. B. Nix, B. Y. Yoo, M. A. Deshusses and N. V. Myung, Electrochemically functionalized single-walled carbon nanotube gas sensor, *Electroanalysis*, 2006, **18**, 1153–1158.
- 201 Y. Zhang, B. R. Bunes, N. Wu, A. Ansari, S. Rajabali and L. Zang, Sensing methamphetamine with chemiresistive sensors based on polythiophene-blended single-walled carbon nanotubes, *Sens. Actuators, B*, 2018, **255**, 1814–1818.
- 202 A. Husain, S. Ahmad and F. Mohammad, Electrical Conductivity and Ammonia Sensing Studies on Polythiophene/MWCNTs Nanocomposites, *Materialia*, 2020, 100868.
- 203 R. Yoo, J. Kim, M. J. Song, W. Lee and J. S. Noh, Nanocomposite sensors composed of single-walled carbon nanotubes and polyaniline for the detection of a nerve agent simulant gas, *Sens. Actuators, B*, 2015, **209**, 444–448.
- 204 C. P. Chang and C. L. Yuan, The fabrication of a MWNTs-polymer composite chemoresistive sensor array to discriminate between chemical toxic agents, *J. Mater. Sci.*, 2009, **44**, 5485–5493.
- 205 S. Ebrahim, R. El-Raey, A. Hefnawy, H. Ibrahim, M. Soliman and T. M. Abdel-Fattah, Electrochemical sensor based on polyaniline nanofibers/single wall carbon nanotubes composite for detection of malathion, *Synth. Met.*, 2014, **190**, 13–19.
- 206 S. Gaikwad, G. Bodkhe, M. Deshmukh, H. Patil, A. Rushi, M. D. Shirsat, *et al.*, Chemiresistive sensor based on polythiophene-modified single-walled carbon nanotubes for detection of NO<sub>2</sub>, *Mod. Phys. Lett. B*, 2015, **29**, 1540046.
- 207 M. Eising, C. E. Cava, R. V. Salvatierra, A. J. G. Zarbin and L. S. Roman, Doping effect on self-assembled films of polyaniline and carbon nanotube applied as ammonia gas sensor, *Sens. Actuators, B*, 2017, **245**, 25–33.
- 208 L. He, Y. Jia, F. Meng, M. Li and J. Liu, Gas sensors for ammonia detection based on polyaniline-coated multi-wall carbon nanotubes, *Mater. Sci. Eng., B*, 2009, **163**, 76–81.
- 209 T. Sarkar, S. Srinives, S. Sarkar, R. C. Haddon and A. Mulchandani, Single-walled carbon nanotube-poly(porphyrin) hybrid for volatile organic compounds detection, *J. Phys. Chem. C*, 2014, **118**, 1602–1610.
- 210 Y. Lu, M. Meyyappan and J. Li, A carbon-nanotube-based sensor array for formaldehyde detection, *Nanotechnology*, 2010, **22**, 055502.
- 211 S. Srivastava, S. S. Sharma, S. Kumar, S. Agrawal, M. Singh and Y. K. Vijay, Characterization of gas sensing behavior of multi walled carbon nanotube polyaniline composite films, *Int. J. Hydrogen Energy*, 2009, **34**, 8444–8450.

